Human Reproduction, Vol.35, No.6, pp. 1391–1410, 2020
Advance Access Publication on June 15, 2020 doi:10.1093/humrep/deaa100

human reproduction

ORIGINAL ARTICLE ***Reproductive biology***

Spatiotemporal changes in mechanical matrisome components of the human ovary from prepuberty to menopause

E. Ouni[1], C. Bouzin[2], M.M. Dolmans[1,3], E. Marbaix[4,5], S. Pyr dit Ruys[6], D. Vertommen[6], and C.A. Amorim[1,*]

[1]Pôle de Recherche en Gynécologie, Institut de Recherche Expérimentale et Clinique, Université Catholique de Louvain, 1200 Brussels, Belgium [2]IREC Imaging Platform (2IP), Institut de Recherche Expérimentale et Clinique, Université Catholique de Louvain, 1200 Brussels, Belgium [3]Gynecology and Andrology Department, Cliniques Universitaires Saint-Luc, 1200 Brussels, Belgium [4]Pathology Department, Cliniques Universitaires Saint-Luc, 1200 Brussels, Belgium [5]Cell Biology Unit, de Duve Institute, Université Catholique de Louvain, 1200 Brussels, Belgium [6]de Duve Institute, Université Catholique de Louvain, Brussels, Belgium

*Correspondence address. Pôle de Recherche en Gynécologie, Institut de Recherche Expérimentale et Clinique, Université Catholique de Louvain, Avenue Mounier 52, bte B1.52.02, 1200 Brussels, Belgium. Tel: +32 (0)2 764 5287; E-mail: christiani.amorim@uclouvain.be

Submitted on November 29, 2019; resubmitted on April 15, 2020; accepted on April 22, 2020

STUDY QUESTION: How do elastic matrisome components change during the lifetime of the human ovary?

SUMMARY ANSWER: The deposition and remodeling of mechanical matrisome components (collagen, elastin, elastin microfibril interface-located protein 1 (EMILIN-1), fibrillin-1 and glycosaminoglycans (GAGs)) that play key roles in signaling pathways related to follicle activation and development evolve in an age- and follicle stage-related manner.

WHAT IS KNOWN ALREADY: The mechanobiology of the human ovary and dynamic reciprocity that exists between ovarian cells and their microenvironment is of high importance. Indeed, while the localization of primordial follicles in the collagen-rich ovarian cortex offers a rigid physical environment that supports follicle architecture and probably plays a role in their survival, ovarian extracellular matrix (ECM) stiffness limits follicle expansion and hence oocyte maturation, maintaining follicles in their quiescent state. As growing follicles migrate to the medulla of the ovary, they encounter a softer, more pliant ECM, allowing expansion and development. Thus, changes in the rigidity of the ovarian ECM have a direct effect on follicle behavior. Evidence supporting a role for the physical environment in follicle activation was provided in clinical practice by ovarian tissue fragmentation, which promoted actin polymerization and disrupted ovarian Hippo signaling, leading to increased expression of downstream growth factors, promotion of follicle growth and generation of mature oocytes.

STUDY DESIGN, SIZE, DURATION: We investigated quantitative spatiotemporal changes in collagen, elastin, EMILIN-1, fibrillin-1 and GAGs from prepuberty to menopause, before conducting a closer analysis of the ECM surrounding follicles, from primordial to secondary stages, in both prepubertal and tissue from women of reproductive age. The study included ovarian tissue (cortex) from 68 patients of different ages: prepubertal ($n = 16$; mean age [±SD]=8 ± 2 years); reproductive ($n = 21$; mean age [±SD]=27 ± 4 years); menopausal with estrogen-based HRT ($n = 7$; mean age [±SD]=58 ± 4 years); and menopausal without HRT ($n = 24$; mean age [±SD]=61 ± 5 years).

PARTICIPANTS/MATERIALS, SETTING, METHODS: Quantitative investigations of collagen and GAG deposition in ovarian tissue throughout a woman's lifetime were conducted by analyzing brightfield images. Characteristic features of collagen fiber content were based on polarized light microscopy, since polarized light changes with fiber thickness. To evaluate the deposition and distribution of elastin, fibrillin-1 and EMILIN-1, multiplex immunofluorescence was used on at least three sections from each patient. Image processing and tailored bioinformatic analysis were applied to enable spatiotemporal quantitative evaluation of elastic system component deposition in the human ovary over its lifetime.

MAIN RESULTS AND THE ROLE OF CHANCE: While collagen levels increased with age, fibrillin-1 and EMILIN-1 declined. Interestingly, collagen and elastin reached their peak in reproductive-age women compared to prepubertal ($P < 0.01$; $P = 0.262$) and menopausal subjects with ($P = 0.706$; $P < 0.01$) and without ($P = 0.987$; $P = 0.610$) HRT, indicating a positive impact of secreted estrogen and hormone treatment on collagen and elastin preservation. Interestingly, HRT appears to affect elastin presence in ovarian tissue, since a significantly higher ($P < 0.05$) proportion of elastin was detected in biopsies from menopausal women taking HRT compared to those not. Higher GAG levels were found in adult ovaries compared to prepubertal ovaries ($P < 0.05$), suggesting changes in tissue ultrastructure and elasticity with age. In this context, elevated GAG values are suspected to participate in hampering formation of the fibrillin-1 network

© The Author(s) 2020. Published by Oxford University Press on behalf of European Society of Human Reproduction and Embryology. All rights reserved.
For permissions, please email: journals.permissions@oup.com

Downloaded from https://academic.oup.com/humrep/article/35/6/1391/5857556 by UCLouvain-SCEB user on 13 June 2022

($r = -0.2475$; $P = 0.04687$), which explains its decline over time. This decline partially accounts for the decrease in EMILIN-1 ($r = 0.4149$; $P = 0.00059$). Closer examination of the ECM surrounding follicles from the primordial to the secondary stage, both before and after puberty, points to high levels of mechanical stress placed on prepubertal follicles compared to the more compliant ECM around reproductive-age follicles, as suggested by the higher collagen levels and lower elastin content detected mainly around primordial ($P < 0.0001$; $P < 0.0001$, respectively) and primary ($P < 0.0001$; $P < 0.001$, respectively) follicles. Such a stiff niche is nonpermissive to prepubertal follicle activation and growth, and is more inclined to quiescence.

LARGE SCALE DATA: Not applicable.

LIMITATIONS, REASONS FOR CAUTION: The duration and form of administered HRT were not considered when studying the menopausal patient group undergoing treatment. Moreover, we cannot exclude interference from other nongynecological medications taken by the study patients on ovarian ECM properties since there is no information in the literature describing the impact of each medication on the ECM. Finally, since the ECM is by definition a very heterogeneous meshwork of proteins, the use of two-dimensional histology could be a limitation. Single time points on fixed tissues could also present limitations, since following ovary dynamics from prepuberty to menopause in the same patient is not feasible.

WIDER IMPLICATIONS OF THE FINDINGS: From a biomechanical perspective, our study revealed important changes to ECM properties dictating the mechanical features of ovarian tissue, in line with the existing literature. Our findings pave the way for possible therapeutic targets at the ECM level in the context of female fertility and ovarian rejuvenation, such as mechanical stimulation, antifibrotic treatments, and prevention or reversion of elastic ECM degradation. Our study also sheds light on the follicle-specific ECM composition that is dependent on follicle stage and age. These data will prove very useful in designing biomimetic scaffolds and tissue-engineered models like the artificial ovary. Indeed, they emphasize the importance of encapsulating each type of isolated follicle in an appropriate biomaterial that must replicate the corresponding functional perifollicular ECM and respect ovarian tissue heterogeneity in order to guarantee its biomimicry.

STUDY FUNDING/COMPETING INTEREST(S): This study was supported by grants from the Fonds National de la Recherche Scientifique de Belgique (FNRS) (C.A.A. is an FRS-FNRS research associate; grant 5/4/150/5 awarded to M.M.D.) and the Université Catholique de Louvain (PhD grant 'Coopération au développement' awarded to E.O.). None of the authors have any competing interests to declare.

Key words: ovary / extracellular matrix / hormone replacement therapy / aging / fertility preservation / mechanobiology

Introduction

The ovary contains a large number of dormant immature follicles, the organ's functional units, each accommodating a single oocyte and residing on the periphery of the ovary. Upon puberty, a group of immature follicles is sequentially activated to resume growth with every reproductive cycle and a single dominant follicle eventually emerges, ovulates, and then involutes to allow selection of the next group of follicles. This process, known as folliculogenesis, makes the human ovary one of the most dynamic tissues in the female body, undergoing repeated cycles of growth and involution throughout her reproductive life.

Although many hormonal and molecular analyses have been conducted to identify the mechanisms underlying ovarian development and folliculogenesis (Adhikari and Liu, 2009; Grive and Freiman, 2015; Hsueh *et al.*, 2015; Filatov *et al.*, 2017; Ford *et al.*, 2019), the role of the extracellular matrix (ECM) in these processes remains unclear. Nevertheless, this last decade has witnessed growing interest in the mechanobiology of the human ovary and the dynamic reciprocity that exists between ovarian cells and their microenvironment (Woodruff and Shea, 2011; Thorne *et al.*, 2015). Indeed, while the localization of primordial (dormant) follicles in the collagen-rich ovarian cortex offers a rigid physical environment that supports follicle architecture and probably plays a role in their survival, ovarian ECM stiffness limits follicle expansion and hence oocyte maturation, maintaining follicles in their quiescent state (Shah *et al.*, 2018). As growing follicles migrate to the medulla of the ovary, they encounter a softer, more pliant ECM, allowing expansion and development. Thus, changes in the rigidity of the ovarian ECM have a direct effect on follicle behavior. This hypothesis was first investigated in *in vitro* experiments (Xu *et al.*, 2006; Hornick *et al.*, 2012; Choi *et al.*, 2014) and substantiated by *in vivo* studies and clinical practice (Kawamura *et al.*, 2016). Evidence supporting a role for the physical environment in follicle activation was provided by Kawamura *et al.* (2013), who proved that ovarian tissue fragmentation promoted actin polymerization and disrupted ovarian Hippo signaling, leading to increased expression of downstream growth factors, promotion of follicle growth and generation of mature oocytes.

This strongly suggests that in addition to well-established biochemical cues (Hsueh *et al.*, 2015), follicle activation depends on the physical environment of the ovary, and any alterations to its normal physical aspects may be implicated in ovarian disorders, such as primary ovarian insufficiency and polycystic ovary syndrome (PCOS) (Wood *et al.*, 2015). Interestingly, therapies for PCOS have included ovarian wedge resection or laser drilling to induce follicle growth (Lunde *et al.*, 2001), but the underlying mechanisms of these disruptive procedures are unclear. So far, our characterization of the biomechanical regulation of the human ovary extends to use of terms such as rigid or soft microenvironment to describe the ovarian ECM, with little focus on the actual elastic system components that give the tissue its intrinsic mechanical features and orchestrate related downstream cell signaling.

The mechanical features of soft tissues are mainly governed by the content and organization of collagen and elastic fibers (Levillain *et al.*,

Downloaded from https://academic.oup.com/humrep/article/35/6/1391/5857556 by UCLouvain-SCEB user on 13 June 2022

2016). Elastic fibers are large ECM structures that provide tissues with recoil needed to undergo repeated stretching and complement the tensile strength of fibrillar collagens. Elastic fibers reside in tissues as a large network composed of two discrete components, namely elastin, the major constituent, and associated microfibrils, mainly fibrillin-1. Elastin microfibril interface-located protein 1 (EMILIN-1) is another glycoprotein present at the interface between amorphous elastin and microfibrils. Glycosaminoglycans (GAGs) participate in the immobilization of water, conferring elasticity to biological tissues and contributing to their homeostasis and osmotic equilibrium (Kurylo *et al.*, 2016). Beyond elastogenesis and mechanical properties, these molecules are linked to a myriad of molecular signaling pathways (Afratis *et al.*, 2012). While they are probably involved in various processes in the ovary, to the best of our knowledge there are no existing studies defining their role in the human ovary and possible association with ovarian follicles.

The goal of this study was therefore to decipher the role of ECM fibers in the human ovary by comparing elastin, EMILIN-1, fibrillin-1 and GAGs in ovarian tissue from prepubertal girls, women of reproductive age and menopausal women both undergoing and not undergoing HRT. Comparisons were made by means of histological staining, immunofluorescence and tissue scanning. Image processing and tailored bioinformatic analysis were used to enable spatiotemporal quantitative evaluation of elastic system component deposition in the human ovary over its lifetime. We also conducted an in-depth analysis of the ECM surrounding preantral follicles before and after puberty in order to link mechanical cues involved in follicle activation with biochemical and hormone regulation.

Materials and methods

Human ovarian tissue

Sixty-eight ovarian tissue samples retrieved from patients of different ages were included in this study (Fig. 1): prepubertal ($n=16$; mean age [±SD]=8 ± 2 years); reproductive-age ($n=21$; mean age [±SD]=27 ± 4 years); menopausal with estrogen-based HRT ($n=7$; mean age [±SD]=58 ± 4 years) and without HRT ($n=24$; mean age [±SD]=61 ± 5 years). All participating adult patients were undergoing laparoscopic surgery for benign gynecologic diseases not affecting the ovaries. Prepubertal tissue was derived from young cancer patients scheduled for ovarian cortex cryopreservation as a fertility preservation strategy, before being subjected to acute gonadotoxic cancer treatments. Sample storage in the biobank of St-Luc's Hospital involved tissue fixation, dehydration and embedding in several paraffin blocks for further investigation by the anatomic pathology department of the institution. Enrolled subjects did not show any alterations to any of the ovaries included in our study, allowing use of residual material (Supplementary Table SI).

Ethics

Use of human ovarian cortex was approved by the Institutional Review Board of the Université Catholique de Louvain on 13 May 2019 (IRB reference 2012/23MAR/125, registration number B403201213872). After obtaining informed consent from all parties, fragments of ovarian tissue were collected.

Morphological selection criteria

All samples used in this study were fixed in 10% neutral buffered formalin overnight at 4°C, before being directly dehydrated and embedded in paraffin. Biopsies were kept in paraffin blocks during collection of study samples and sectioned (serial sections of 5 µm) just before analysis to better preserve their antigen epitopes. The cortical layer of each ovarian sample was evaluated, and every fourth slide was stained with hematoxylin-eosin (Merck, Darmstadt, Germany) for morphological analysis and follicle classification. This step enabled selection of tissue sections with high and comparable follicle numbers within prepubertal and reproductive-age group for further comparative analysis. A total of three to five slides were examined from each sample.

Hematoxylin-eosin staining was also used to select only cortical sections and exclude slides containing the tunica albuginea or medullary compartment to avoid any bias in ECM characterization. The medulla contains many large blood vessels and lacks the swirling, highly cellular appearance typical of the ovarian cortex. These characteristic features, in addition to assistance from an experienced histologist, helped ensure that the tissue analyzed was solely from the cortex. The remaining slides (Superfrost® Plus slides, Menzel-Glaser, Braunschweig, Germany) were kept for immunofluorescence and additional histological staining (Fig. 1)

Follicle classification was based on the following criteria defining: primordial follicles containing flattened granulosa cells surrounding the oocyte; primary follicles with one layer of cuboidal granulosa cells; and secondary follicles with at least two layers of granulosa cells and no antrum. Follicles with binuclear oocytes and those showing disrupted integrity and signs of degeneration (pyknotic oocyte nuclei, shrunken ooplasm and/or disorganized granulosa cells) were all excluded from the study.

Histological staining

Five-µm-thick paraffin sections were deparaffinized, rehydrated and treated with a saturated picric acid solution containing 1.3% Sirius Red for 1 h at room temperature. GAGs were identified by Alcian blue staining at pH 2.5 (Bio-Optica, Milan, Italy), as described (Hayat, 1993). Alcian blue staining at pH 2.5 selectively labels carboxylated and sulfated GAGs, based on its positive charge attracted to negative structures (e.g. acidic sugars forming the GAGs). Its bulkiness prevents its diffusion toward other highly negative structures in tissue, such as chromatin and Nissl substance (Kiernan, 2006).

Human small intestine was used as a positive control to monitor Alcian blue staining quality (Supplementary Fig. S1). Slides were digitized at X20 magnification with a Leica SCN400 Slide Scanner (Leica, Heerbrugg, Switzerland).

Acquisition of collagen birefringence

In addition to brightfield observations, sections stained with Sirius Red were observed under polarized light using a Nikon Eclipse Ci microscope, and captured with a Leica DFC450 camera equipped with filters to provide circularly polarized illumination. Filters were aligned so that the background in the field of view was as dark as possible, as

Downloaded from https://academic.oup.com/humrep/article/35/6/1391/5857556 by UCLouvain-SCEB user on 13 June 2022

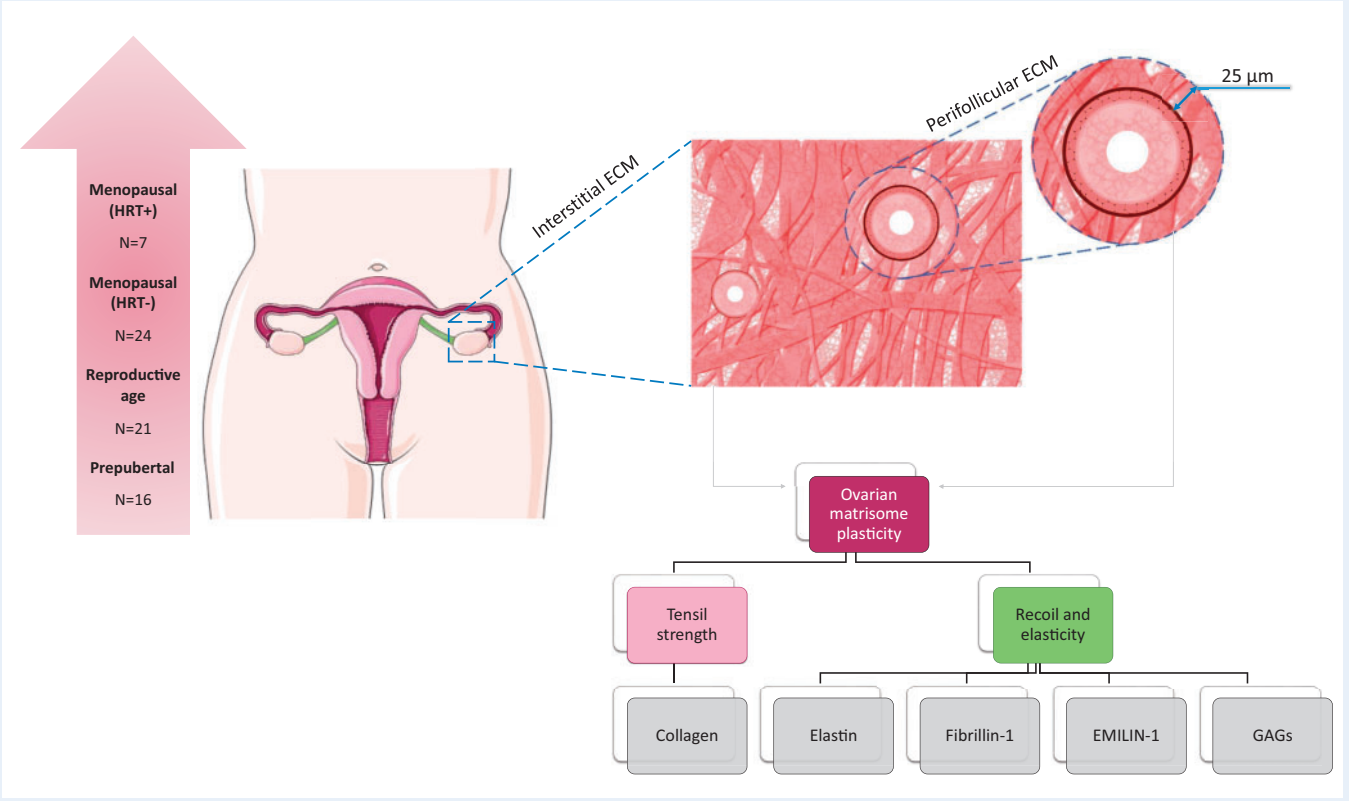


Figure 1 Schematic of the study of elastic matrisome components in human ovary. This study investigates the elastic matrisome components that control ovarian tissue plasticity: collagen, which is associated with tensile strength; and elastin, elastin microfibril interface-located protein (EMILIN-1), fibrillin-1 and glycosaminoglycans (GAGs), which are all associated with tissue recoil and elasticity. First, we studied their quantitative spatiotemporal changes from prepuberty to menopause (with and without HRT [HRT+/HRT−]) in the interstitial extracellular matrix (ECM), before conducting a closer analysis of the perifollicular ECM surrounding follicles from primordial to secondary stages in both prepubertal and reproductive-age tissue. The female genital apparatus illustration was created using Servier Medical Art templates, which are licensed under a Creative Commons Attribution 3.0 Unported License (https://smart.servier.com).

previously reported (Rich and Whittaker, 2005). Objective lenses set at X20 and X40 magnification were used to capture global and perifollicular ECM, respectively.

Each area of interest was captured under polarized and brightfield light in order to obtain a morphological readout and enable identification of follicle developmental stage. Pictures at the same magnification were taken under the same conditions (exposure, gain, saturation and gamma).

Immunofluorescence

To evaluate elastin, fibrillin-1 and EMILIN-1 deposition and distribution, multiplex immunofluorescence was used on at least three sections from each patient, following a previously described protocol (Aboubakar Nana *et al.*, 2019). All antibodies were tested separately with 3,3′-diaminobenzidine (DAB) and immunofluorescence on successive slides, before conducting multiplex immunofluorescence to ensure that no cross-reactivity between antibodies is present and the signal is not affected by the tissue processing steps (Supplementary Fig. S2).

After deparaffinization in Histosafe (Yvsolab SA, Beerse, Belgium) and ethanol, autofluorescence was quenched by 10-min incubation in 50 mM NH_4Cl, and endogenous peroxidase inhibition was achieved after 30 min in 0.3% H_2O_2. Sections were then subjected to water bath antigen retrieval in 10 mM citrate buffer (pH 5.7) containing 0.1% Triton or Tris-EDTA buffer (pH9.0), before blocking of nonspecific antigen binding sites (Tris-buffered saline (TBS) solution containing 10% normal goat serum and 1% bovine serum albumin (BSA)). The first primary antibody was incubated overnight at 4°C in a humid chamber in TBS containing 1% BSA and 0.1% Tween-20 and detected by corresponding horseradish peroxidase (HRP)-conjugated secondary antibodies (Envision, Dako, Glostrup, Denmark) for 1 h at room temperature. HRP was then visualized by tyramide signal amplification using Alexa Fluor-conjugated tyramides (Invitrogen Carlsbad, CA, USA). After one more citrate buffer antigen retrieval step, the same protocol was applied with other primary antibodies and different Alexa Fluor-conjugated tyramides. In all, three sequential reactions were performed with anti-elastin, anti-fibrillin-1 and anti-EMILIN-1 (Table I). Finally, nuclei were counterstained with Hoechst 33342 (Thermo Fisher Scientific, Waltham, MA, USA) and mounted with HIGHDEF IHC fluoromount (Enzo, New York, USA). Negative controls were conducted by adding rabbit IgG (Dako, Carpinteria, USA) instead of the primary antibody, while human testis was used for positive controls of all tested antibodies (Supplementary Fig. S2). Stained slides

Downloaded from https://academic.oup.com/humrep/article/35/6/1391/5857556 by UCLouvain-SCEB user on 13 June 2022

Table I Primary antibodies and respective parameters.

Antigen	Primary antibody				Secondary antibody			TSA Fluochrome
	Concentration (μg/ml)	Incubation	Company	Catalog number	Polymer HRP	Company	Catalog number	
Elastin	2.20 (1/250)	0/N 4°C	Abcam	EPR 20603	Anti-rabbit	Agilent/Dako	K4003	AF488
Fibrillin-1	0.50 (1/200)	0/N 4°C	Sigma	HPA 017759				AF555
EMILIN-1	3 (1/100)	0/N 4°C	Sigma	HPA 002822				AF647

HPR, horseradish peroxidase; TSA, tyramine signal amplification; EMILIN-1, elastin microfibril interface 1.

Table II Number of follicles selected for analysis of the perifollicular extracellular matrix.

	Primordial follicles		Primary follicles		Secondary follicles	
	Prepubertal tissue	Reproductive age tissue	Prepubertal tissue	Reproductive age tissue	Prepubertal tissue	Reproductive age tissue
Collagen (BF)	841	241	196	161	30	48
Collagen (PL)	128	64	39	39	11	23
Elastin	826	260	310	198	25	13
Fibrillin-1	826	260	310	198	25	13
EMILIN-1	826	260	310	198	25	13
GAGs	217	238	182	160	18	30

Number of human follicles selected for analysis of the perifollicular extracellular matrix. Brightfield (BF) and polarized light (PL) microscopy were used for detection of collagen. Elastin, fibrillin-1 and EMILIN-1 were detected by multiplex immunofluorescence, so their evaluation was conducted over the same perifollicular areas, explaining the identical number of selected follicles. Carboxylated and sulfated glycosaminoglycans (GAGs) were selectively labeled by Alcian blue staining (pH 2.5).

were digitized by automated whole-slide image capture with a Pannoramic 250 Flash III scanner (3DHISTECH Ltd, Budapest, Hungary).

Digital image analysis

To ensure reproducible and objective results, computer-assisted quantification of immunofluorescence labeling and histological staining was carried out with Oncotopix, version 2017.2 (Visiopharm, Hoersholm, Denmark) (Supplementary Fig. S3). Tailored software applications were developed by our team to detect tissue regions of interest (ROIs); quantify ROI area; and measure the stained area within a given ROI. Vessels, oocytes and artifacts were manually discarded from ROIs.

Computer-assisted quantification of staining (brightfield: GAGs, Sirius Red) and immunostaining (fluorescence: elastin, EMILIN-1, fibrillin-1) was based on the following equation:

$$\% \text{ stained area} = \text{stained area} \times 100/\text{ROI area}.$$

The same quantification was applied in a concentric region (25-μm-thick) surrounding follicles after their manual delineation and separation into primordial, primary and secondary, based on criteria described in the 'Morphological selection criteria' section (Supplementary Fig. S3, Table II).

Collagen content characterization was based on the birefringence of Sirius Red stained sections under polarized light. It is known that the color of collagen fibers stained with Sirius Red and viewed under polarized light depends on fiber thickness and packing, with polarization colors ranging from green to yellow, orange and red according to their increase in diameter and packing density (Dayan *et al.*, 1989).

To establish proportions of different polarization colors, we used a macro program developed in-house on Fiji software (Schindelin *et al.*, 2012) to automate the quantification (Supplementary Fig. S4, Table II). This macro program determines the total area of polarized pixels using the color threshold tool on Fiji and classifies them into three categories based on the hue histogram. We used a modification of hue definitions applied by MacKenna *et al.* (1994): red 2–9, yellow/orange 10–38, green 24–135. Results were expressed as:

$$\% \text{ polarized collagen} = \text{green}-, \text{yellow/orange}- \text{ or red} - \text{positive area} \times 100/\text{total positive area}.$$

All quantifications were performed blinded to group assignment.

Statistical analysis

Data are presented as mean ± SEM and were calculated using the GraphPad Prism software package, version 8.0 (San Diego, CA, USA).

Downloaded from https://academic.oup.com/humrep/article/35/6/1391/5857556 by UCLouvain-SCEB user on 13 June 2022

Descriptive analyses of values (Dagostino and Pearson or Shapiro–Wilk normality tests) were conducted before each evaluation to select the appropriate statistical test. One-way ANOVA or the Kruskal–Wallis test followed by *post hoc* multiple comparisons using Dunn's test were applied when required to compare interstitial ECMs. Differences in perifollicular ECMs in each of the prepubertal and reproductive-age ovaries were evaluated based on two-way ANOVA or Kruskal–Wallis tests, depending on data distribution. The multiple Student's *t*-test or Mann–Whitney test were used to compare prepubertal and reproductive-age perifollicular ECMs at the same developmental stage. Differences were considered significant at values of $P < 0.05$. Spearman's correlation was applied to measure EMILIN-1/fibrillin-1 and GAG/fibrillin-1 interdependence.

Results

Collagen

Quantitative investigation of collagen deposition in ovarian tissue throughout a woman's lifetime was carried out by analyzing brightfield images. Characteristic features of collagen fiber content were based on polarized light microscopy, since polarized light changes with fiber thickness, as described above.

Collagen levels increase with age

Digital image analysis of ovarian tissue from prepubertal, reproductive-age and menopausal women with or without HRT allowed comparison of collagen deposition levels. Quantification was based on Sirius Red staining acquired on brightfield images (Supplementary Fig. S3). Our results showed a continual increase in collagen levels from prepuberty to menopause, with a significant difference between prepubertal tissue and reproductive-age subjects ($P < 0.01$) as well as with menopausal subjects under HRT ($P < 0.05$) (Fig. 2A and B). Maintenance of collagen levels between reproductive-age subjects and menopausal women without HRT and the absence of any statistically significant difference ($P = 0.706$) clearly demonstrate that collagen reaches its peak at reproductive age (Fig. 2A and B).

Collagen fibers evolve with age

While analyses of Sirius Red staining with brightfield microscopy showed rising collagen fiber deposition with age, it was paramount to look more closely at collagen fiber thickness and its evolution with age. Polarized light microscopy was used once again to inspect the same slides stained with Sirius Red, and revealed that red fibers (the thickest) are the least abundant in human ovarian cortex at any age and represent <7% of total collagen. Interestingly, the reproductive-age group retained the highest proportion of thick collagen fibers of all groups. Thin fibers (green) and average-size fibers (orange and yellow) were found at equivalent rates (~48%) in all groups except prepubertal, where we detected the highest percentage of thin fibers ($61 \pm 3.1\%$) and the lowest percentage of average fibers ($35 \pm 2.8\%$) (Fig. 2A–C).

ECM surrounding prepubertal follicles is the richest in collagen

Although collagen levels do not appear to change with follicle development in either young or adult patients, we encountered significantly higher collagen content in the microenvironment of both primordial ($P < 0.0001$) and primary ($P < 0.0001$) follicles derived from prepubertal ovarian tissue compared to reproductive-age tissue (Fig. 3A and B).

Collagen fiber content in ECM surrounding primordial follicles differs between prepubertal and reproductive-age ovaries

Closer investigation of the microenvironment of primordial follicles at different ages revealed a significantly higher proportion of thick fibers ($P < 0.001$) and lower levels of intermediate ($P < 0.001$) and thin ($P < 0.001$) fibers at prepuberty. High levels of thick collagen fibers seen in perifollicular areas of prepubertal ovaries do not appear to significantly change during early folliculogenesis. On the other hand, a significant decrease in thick collagen fibers was observed in the perifollicular ECM of reproductive-age ovaries, from primary to secondary follicles (Fig. 3A–C).

Elastin

It is known that elastin fibers enable tissues to go through repeated stretching and contraction, so we could hypothesize that elastin plays a major role in a dynamic organ like the ovary. For this reason, we studied its presence and localization in the ECM of different ovary age groups.

Elastin concentrations are affected by aging and HRT

Levels of elastin were as high as 5% in human ovarian tissue, but its density varies according to age. Although we saw a moderate increase from prepubertal to reproductive-age tissue, elastin levels fell dramatically in menopausal women not using HRT ($P < 0.01$) (Fig. 4). Interestingly, hormone substitutes appear to affect elastin presence in ovarian tissue, since a significantly higher ($P < 0.05$) proportion of elastin was detected in biopsies from menopausal women taking HRT compared to those who were not (Fig. 4).

Perifollicular ECM in prepubertal ovaries contains the least elastin

In-depth analysis of the perifollicular ECM revealed significantly lower elastin content around primordial ($P < 0.0001$) and primary ($P < 0.001$) follicles in prepubertal ovarian tissue compared to reproductive-age counterparts (Fig. 5).

Fibrillin-1

Fibrillin-1 microfibrils are associated with elastin and play an important role in the mechanical properties of biological tissues, with implication in biochemical pathways. Fibrillin-1 levels were therefore investigated in ovarian ECM and related to age, follicle stage and hormones.

Fibrillin-1 levels are age-dependent

Fibrillin-1 levels do not change from prepuberty to reproductive age, but drop by half upon menopause. However, by contrast with elastin, fibrillin-1 deposition was not found to be affected by HRT administration (Fig. 6).

Fibrillin-1 levels do not vary in a similar manner in the perifollicular ECM of prepubertal and reproductive-age ovarian tissue

While fibrillin-1 levels did not significantly change during reproductive age in the perifollicular ECM overall, levels rose in prepubertal ovarian tissue following follicle activation ($P < 0.001$). A higher proportion of fibrillin-1 was detected in the ECM surrounding primary ($P < 0.001$)

Downloaded from https://academic.oup.com/humrep/article/35/6/1391/5857556 by UCLouvain-SCEB user on 13 June 2022

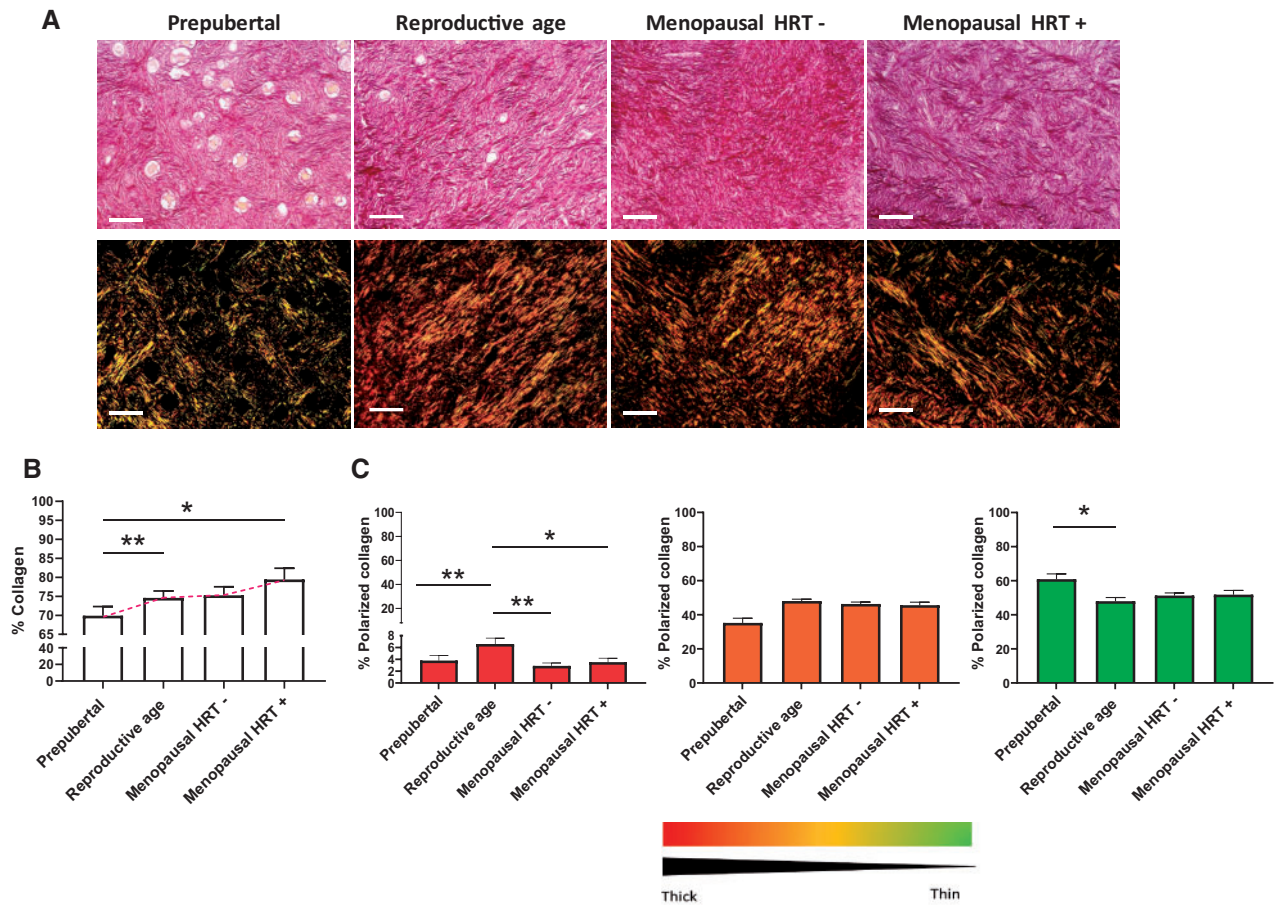


Figure 2 Spatiotemporal evolution of collagen deposition in the ovarian interstitial ECM under brightfield and polarized light microscopy. (**A** and **B**) Quantitative investigation of collagen deposition in ovarian tissue throughout a woman's lifetime was carried out by analyzing brightfield images, which revealed that collagen levels in the human ovary reach a peak at reproductive age (75% ± 1.8). (**C**) Characteristic features of collagen fiber content were based on collagen birefringence observed under polarized light microscopy, since polarized light changes according to fiber thickness: thick fibers (red); average-size fibers (yellow/orange); and thin fibers (green). Thin fibers and average-size fibers were found at equivalent rates (∼48%) in all groups except prepubertal tissue, where we detected the lowest rate of average-size fibers (35% ± 2.8) and the highest rate of thin fibers (61% ± 3.1). These decrease in reproductive-age subjects in favor of thicker collagen fibers. The represented data included analysis of ovarian tissue from 68 patients: prepubertal ($n = 16$); reproductive ($n = 21$); menopausal with estrogen-based HRT ($n = 7$); and menopausal without HRT ($n = 24$). One-way ANOVA (*post hoc*: Tukey) and Kruskal–Wallis (*post hoc*: Dunn) tests were, respectively, used to compare collagen content and fiber thickness between groups (*$P < 0.05$ and **$P < 0.01$). Results are presented as mean ± SEM. Scale bars: 100 µm.

follicles in prepubertal ovaries compared to reproductive-age tissue (Fig. 7).

Elastin microfibril interface-located protein 1

EMILIN-1 is a key glycoprotein associated with the ECM elastic system and implicated in elastogenesis, among other functions (Zanetti *et al.*, 2004). It is therefore another pivotal element in the elastic system, whose spatiotemporal deposition in the human ovary needed investigation.

EMILIN-1 levels fluctuate with age

At prepuberty, around 30% of the ovarian ECM surface area is composed of EMILIN-1, which increases slightly after puberty, only to decrease again at menopause (Fig. 8). Contrary to the positive effect that HRT has on elastin at menopause, no significant difference in EMILIN-1 levels was found between menopausal patients with or without HRT ($P = 0.683$). It is important to stress that the distribution of EMILIN-1 was highly heterogeneous in ovarian tissue and between patients, which hampered detection of statistically significant results, despite a clear tendency. Indeed, the ECM is a very heterogeneous protein meshwork that varies even within the same biological sample (Malandrino *et al.*, 2018). Therefore, it was no surprise to find a wide range of expression of EMILIN-1 in large tissue areas like interstitial ECM.

Perifollicular ECM in prepubertal ovaries contains low levels of EMILIN-1

The limited area of perifollicular ECM (25-µm-thick perimeter) showed considerably less heterogeneity in perifollicular ROIs compared to

Downloaded from https://academic.oup.com/humrep/article/35/6/1391/5857556 by UCLouvain-SCEB user on 13 June 2022

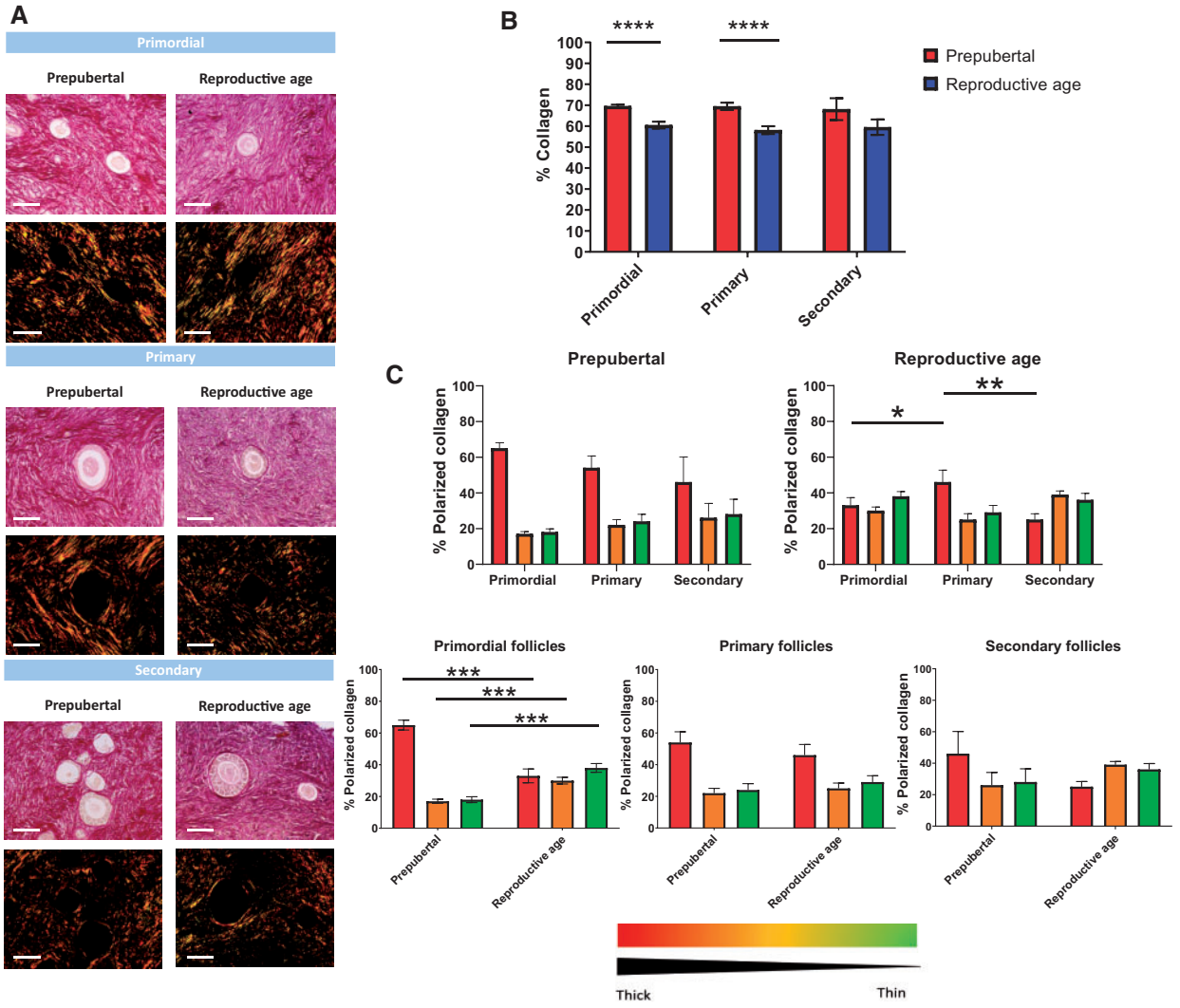


Figure 3 Comparison of collagen content and cross-linking between prepubertal and reproductive-age perifollicular ECM during early folliculogenesis. (**A** and **B**) Greater accumulation of collagen was detected in the microenvironment of both primordial and primary follicles derived from prepubertal ovarian tissue compared to reproductive-age tissue. (**C**) Investigation of the microenvironment of primordial follicles at different ages under polarized light revealed a significantly higher proportion of thick fibers and lower levels of intermediate and thin fibers at prepuberty. A significant decrease in thick collagen fibers was also observed around reproductive-age ovaries, from the primary to the secondary follicle stage. The Kruskal–Wallis test and multiple Student's *t*-test with the Holm–Sidak method for multiple comparison correction were, respectively, used to compare collagen amounts and fiber thickness between groups. The represented data included analysis of follicles from prepubertal ($n = 16$) and reproductive age tissues ($n = 21$). The comparison of perifollicular ECM at prepubertal versus reproductive age under bright field included primordial ($n = 841$ vs $n = 241$), primary ($n = 196$ vs $n = 161$) and secondary ($n = 30$ vs $n = 48$) follicles. The comparison of perifollicular ECM at prepubertal versus reproductive age under polarized light included primordial ($n = 128$ vs $n = 64$), primary ($n = 39$ vs $n = 39$) and secondary ($n = 11$ vs $n = 23$) follicles. Two-way ANOVA (*post hoc*: Tukey) was used to compare collagen thickness between follicle stages in each group (**$P<0.01$, ***$P<0.001$ and ****$P<0.0001$). Results are presented as mean ± SEM. Scale bars: 50 µm.

interstitial ECM. Indeed, lower amounts of EMILIN-1 were detected in the perifollicular ECM of prepubertal ovarian tissue, reaching statistical significance in primordial follicles ($P < 0.05$). In both prepubertal and reproductive-age patients, we observed a decline in EMILIN-1 levels following follicle activation (Fig. 9), but it was only significant in reproductive-age ovaries ($P < 0.01$).

Glycosaminoglycans

Thanks to their affinity for water, GAGs provide a mechanism of resistance to deformation. We therefore investigated their density in ovarian tissue in order to understand their involvement in the mechanical properties of the human ovary.

Downloaded from https://academic.oup.com/humrep/article/35/6/1391/5857556 by UCLouvain-SCEB user on 13 June 2022

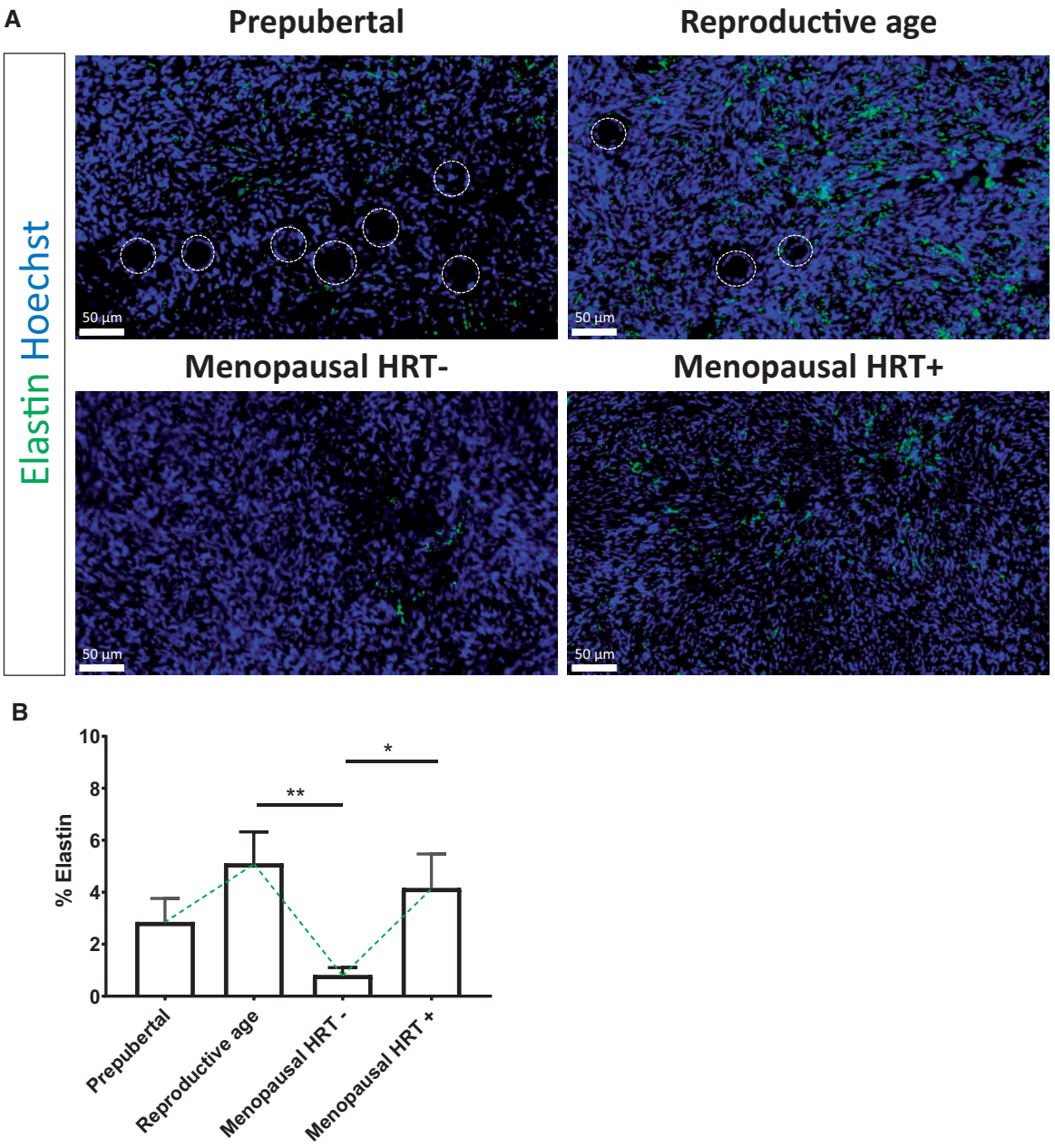


Figure 4 Spatiotemporal elastin synthesis and coacervation in the ovarian interstitial ECM. (**A**) Immunofluorescent staining of tissue sections for elastin (green) and counterstaining with Hoechst (blue) for nuclear observation. (**B**) Levels of elastin were as high as 5% in human ovarian tissue, but its density is known to vary according to age and reaches its peak at reproductive age, before drastically declining at menopause (HRT−) when estrogen levels are almost zero. On the other hand, elastin levels remained comparable to those at reproductive age in menopausal women taking hormone replacement therapy (HRT+), revealing possible *de novo* synthesis of elastin under estrogen. The represented data included analysis of ovarian tissue from 68 patients: prepubertal ($n = 16$); reproductive ($n = 21$); menopausal with estrogen-based HRT ($n = 7$); and menopausal without HRT ($n = 24$). The Kruskal–Wallis (*post hoc*: Dunn) test was used to compare elastin levels between age groups (*$P < 0.05$, **$P < 0.01$). Drawn circles highlight the presence of preantral follicles. Results are presented as mean ± SEM. Scale bars: 50 µm.

GAG levels increase with age

Comparison between different groups revealed a significant difference between prepubertal ovarian ECM and both reproductive-age ($P < 0.01$) and menopausal ovarian ECM with ($P < 0.001$) and without ($P < 0.05$) HRT (Fig. 10).

GAG content is different in the perifollicular ECM of prepubertal and reproductive-age ovarian tissue

While levels of GAGs fell significantly ($P < 0.001$) in the perifollicular microenvironment of prepubertal patients during early folliculogenesis, they remained stable at reproductive age from the primary to the

Downloaded from https://academic.oup.com/humrep/article/35/6/1391/5857556 by UCLouvain-SCEB user on 13 June 2022

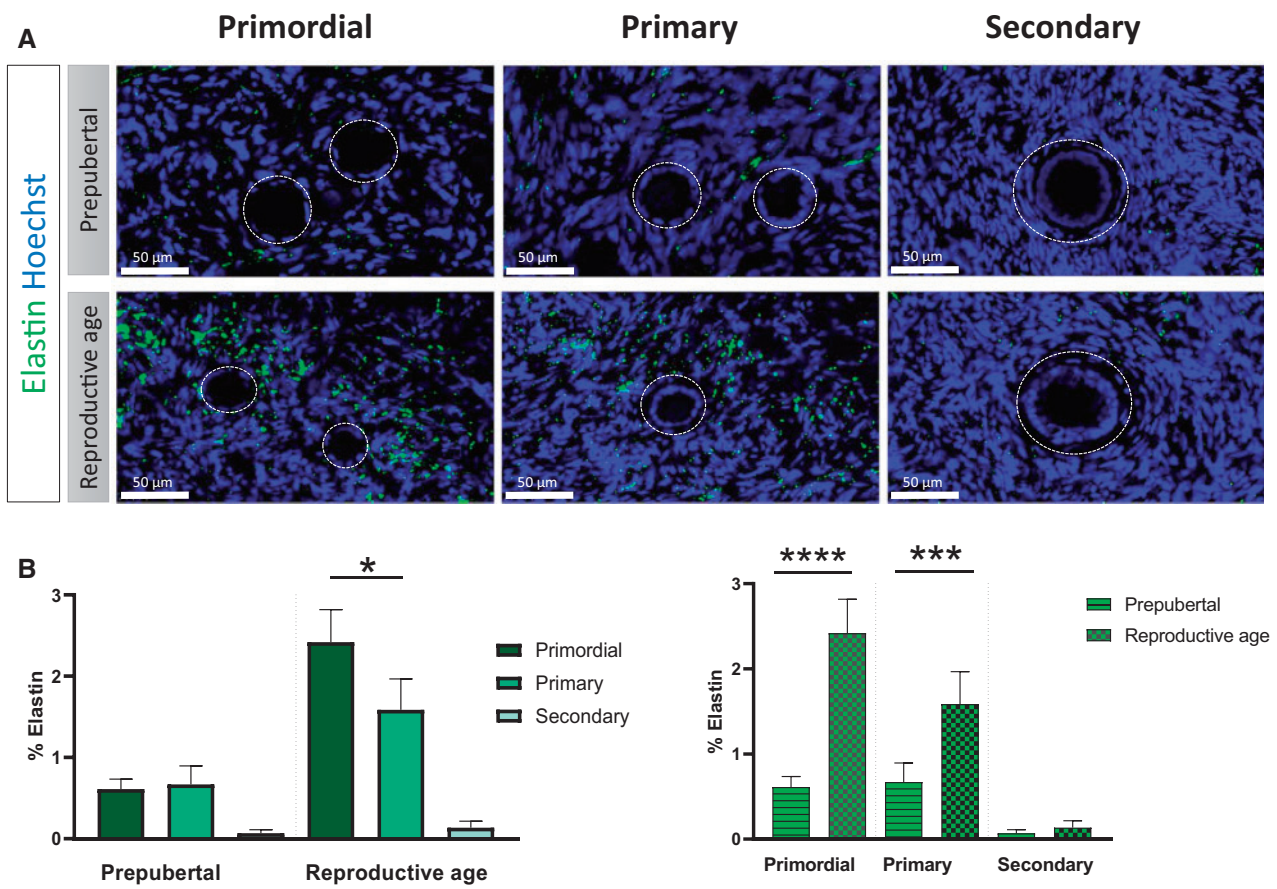


Figure 5 Comparison of elastin distribution and deposition between prepubertal and reproductive-age perifollicular ECM during early folliculogenesis. (**A**) Immunofluorescent staining of tissue sections for elastin (green) and counterstaining with Hoechst (blue) for nuclear observation. (**B**) Lower elastin content was observed around prepubertal primordial and primary follicles compared to their reproductive-age counterparts, indicating a less compliant environment. The represented data included analysis of follicles from prepubertal ($n = 16$) and reproductive age tissues ($n = 21$). The comparison of perifollicular ECM at prepubertal versus reproductive age included primordial ($n = 826$ vs $n = 260$), primary ($n = 310$ vs $n = 198$) and secondary ($n = 25$ vs $n = 13$) follicles. The Kruskal–Wallis (*post hoc*: Dunn) test was used to compare elastin levels between follicle stages in each group, and the Mann–Whitney test to compare prepubertal and reproductive-age follicles at the same developmental stage (*$P<0.05$, ***$P<0.001$, ****$P<0.0001$). Drawn circles highlight the presence of preantral follicles. Results are presented as mean ± SEM. Scale bars: 50 µm.

secondary stage. By comparing follicles of the same stage from prepubertal and adult patients, we found a significantly higher GAG content in the microenvironment of primary ($P < 0.0001$) and secondary ($P < 0.0001$) follicles in ovarian tissue from reproductive-age women. However, at the primordial stage, no difference was detected between young and adult ovarian tissue (Fig. 11).

Discussion

In recent years, we have witnessed a new dawn in mechanobiology dictating that mechanical forces generated within tissues can provide regulatory signals that are just as important as those conveyed by chemicals and genes (Mammoto *et al.*, 2013). This fact is reflected in the field of fertility preservation by numerous theories (Woodruff and Shea, 2011; Choi *et al.*, 2014; Thorne *et al.*, 2015), and lately by the work of Kawamura *et al.* (Kawamura *et al.*, 2013; Kawashima and Kawamura, 2018), which associates ovarian follicle activation to mechanical stress release. However, the real players orchestrating mechanical behavior in the ovary remain unknown. In this study, we investigated quantitative spatiotemporal changes in microstructural elastic components in interstitial and perifollicular ECM, looking to establish a potential connection between these molecules, follicle activation and early development.

What is behind the biomechanical properties of human ovarian tissue?

Our quantification of collagen and elastin deposition in the ovary throughout a woman's lifetime revealed progressive accumulation of these proteins in the ovarian ECM of prepubertal to reproductive-age subjects, as expected in late-stage tissue development (Oomen *et al.*, 2018). Our data demonstrate that collagen reaches its peak during

Downloaded from https://academic.oup.com/humrep/article/35/6/1391/5857556 by UCLouvain-SCEB user on 13 June 2022

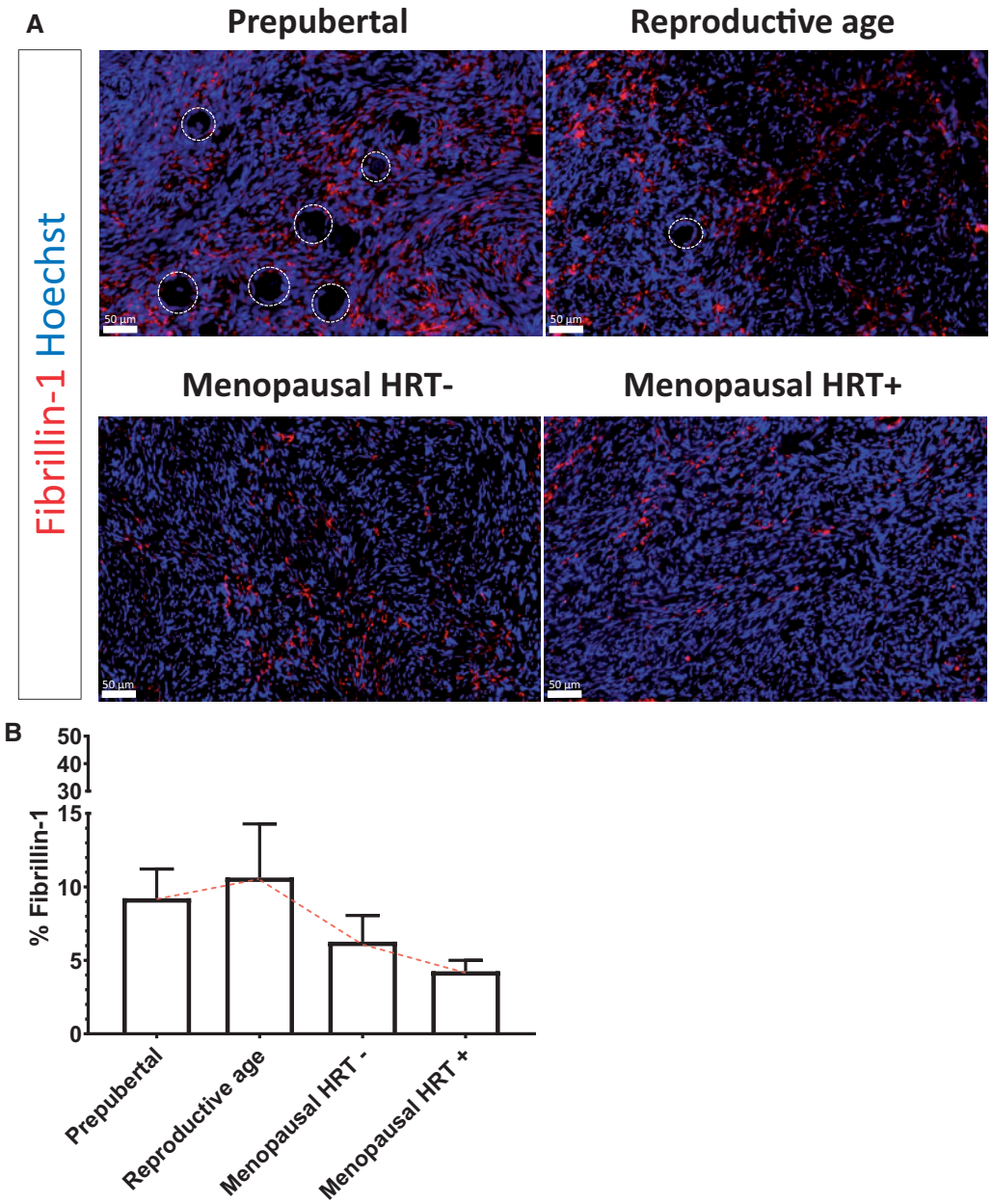


Figure 6 Spatiotemporal evolution of fibrillin-1 deposition in the ovarian interstitial ECM. (**A**) Immunofluorescent staining of tissue sections for fibrillin-1 (red) and counterstaining with Hoechst (blue) for nuclear observation. (**B**) Fibrillin-1 levels did not change from prepuberty to reproductive age, but dropped by half upon menopause. By contrast with elastin, fibrillin-1 deposition is not affected by HRT administration. The represented data included analysis of ovarian tissue from 68 patients: prepubertal ($n = 16$); reproductive ($n = 21$); menopausal with estrogen-based HRT ($n = 7$); and menopausal without HRT ($n = 24$). The Kruskal–Wallis (*post hoc*: Dunn) test was used to compare fibrillin-1 levels between age groups (*$P < 0.05$). Drawn circles highlight the presence of preantral follicles. Results are presented as mean ± SEM. Scale bars: 50 µm.

reproductive age in healthy ovaries. Interestingly, we observed a significant difference in collagen levels in the ovary before and after puberty, and also within menopausal ovarian tissue under HRT, pointing to the involvement of steroids in collagen deposition (Supplementary Video). We can speculate that estrogen is implicated in the activation of lysyl oxidase (LOX) and lysyl oxidase-like 1 (LOXL1), two enzymes governing collagen cross-linking and leading to dense deposition of collagen (Sanada *et al.*, 1978). Our results using polarized light microscopy also corroborate our hypothesis that estrogen is involved in collagen cross-linking in ovarian tissue, as demonstrated by the decrease in thin fibers

Downloaded from https://academic.oup.com/humrep/article/35/6/1391/5857556 by UCLouvain-SCEB user on 13 June 2022

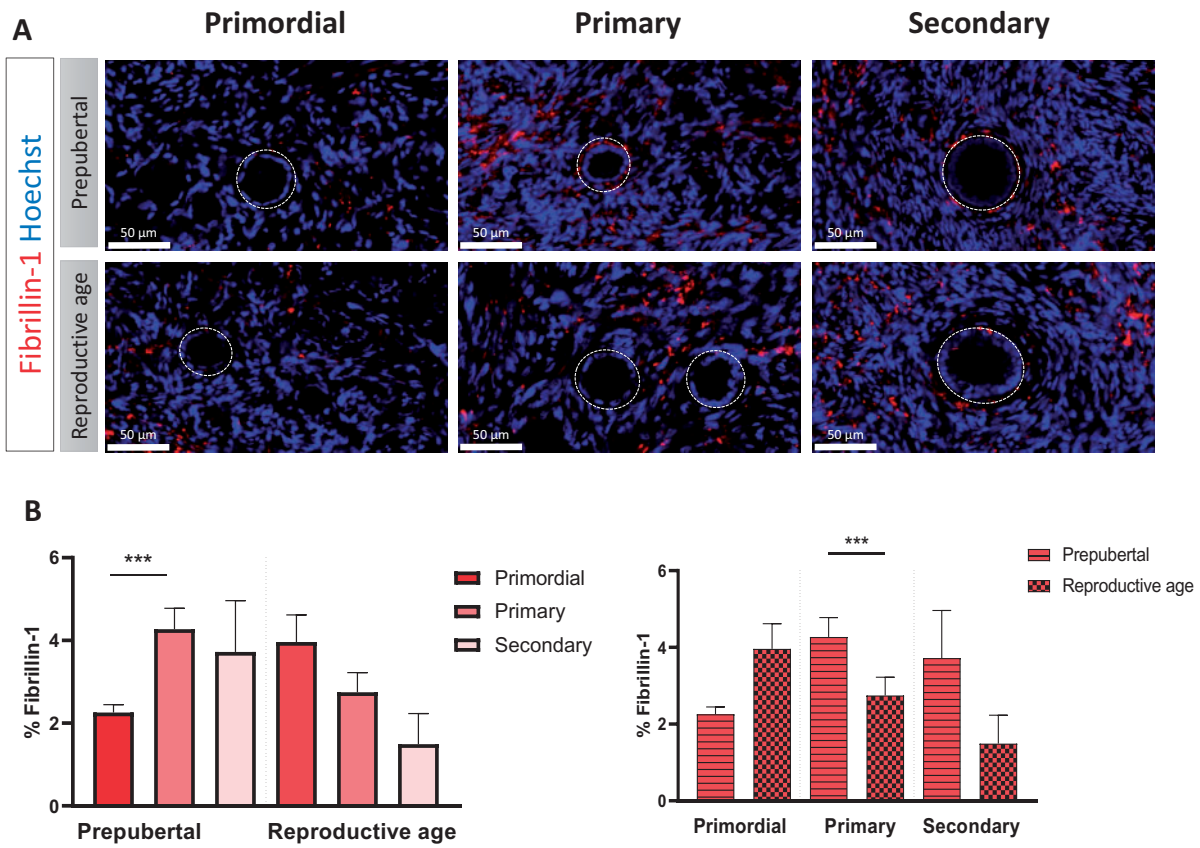


Figure 7 Comparison of fibrillin-1 distribution and deposition between prepubertal and reproductive-age perifollicular ECM during early folliculogenesis. (**A**) Immunofluorescent staining of tissue sections for fibrillin-1 (red) and counterstaining with Hoechst (blue) for nuclear observation. (**B**) While fibrillin-1 levels did not significantly change during reproductive age in the perifollicular ECM overall, during early folliculogenesis its levels increased in prepubertal ovarian tissue, mainly following follicle activation. The represented data included analysis of follicles from prepubertal ($n = 16$) and reproductive age tissues ($n = 21$). The comparison of perifollicular ECM at prepubertal versus reproductive age included primordial ($n = 826$ vs $n = 260$), primary ($n = 310$ vs $n = 198$) and secondary ($n = 25$ vs $n = 13$) follicles. The Kruskal–Wallis (*post hoc*: Dunn) test was used to compare fibrillin-1 levels between follicle stages in each group, and the Mann–Whitney test to compare prepubertal and reproductive-age follicles at the same developmental stage (***$P < 0.001$). Drawn circles highlight the presence of preantral follicles. Results are presented as mean ± SEM. Scale bars: 50 µm.

and increase in thick fibers, mainly in reproductive-age ovaries, that are modulated by physiological estrogen levels. Estrogen also has a role in the mechanical properties of ovarian tissue through its impact on elastin production, as evidenced by the significant decline in elastin in menopausal ovaries without HRT. It is widely acknowledged that elastin synthesis in human starts from late fetal stages to the early postnatal period, gradually decreasing and ceasing in adults (Swee *et al.*, 1995). However, our study indicates that when estrogen is present, elastin continues to be synthesized. Immunofluorescence analyses demonstrate that elastin not only remains at similar levels in adult ovaries compared to their prepubertal counterparts, but also can be synthesized *de novo* under the influence of HRT in menopausal ovaries. Although ovarian tissue is known to be very elastic, especially at reproductive age, our results on elastin provide more insights into this common belief. Indeed, elastin levels in the ovarian cortex do not exceed 5%, while elastin constitutes about 28–32% of major blood vessels, 30–57% of the aorta, 50% of elastic ligaments, 3–7% of lung tissue and 2–3% of the dry weight of skin, where elasticity and flexibility are of major importance (Lescan *et al.*, 2018).

In addition to collagen and elastin, microfibrils play a key role in mechanoregulation and contribute significantly to the long-term stability of elastic fibers, serving as a scaffold for elastin deposition (Marque *et al.*, 2001). Among the three known fibrillin isoforms, fibrillin-1 is the most abundant microfibril isoform in mature tissues, specifically in the human ovary (Bastian *et al.*, 2016; Ouni *et al.*, 2019). Our spatiotemporal follow-up of fibrillin-1 showed a tendency toward a progressive downturn in availability from prepuberty to menopause (with and without HRT), which may be one of the reasons for elastin decline with age. Hence, in contrast to its impact on collagen and elastin, HRT does not have any effect on fibrillin-1 synthesis or coacervation, which might harm the integrity of elastin synthesized by menopausal women taking HRT.

Downloaded from https://academic.oup.com/humrep/article/35/6/1391/5857556 by UCLouvain-SCEB user on 13 June 2022

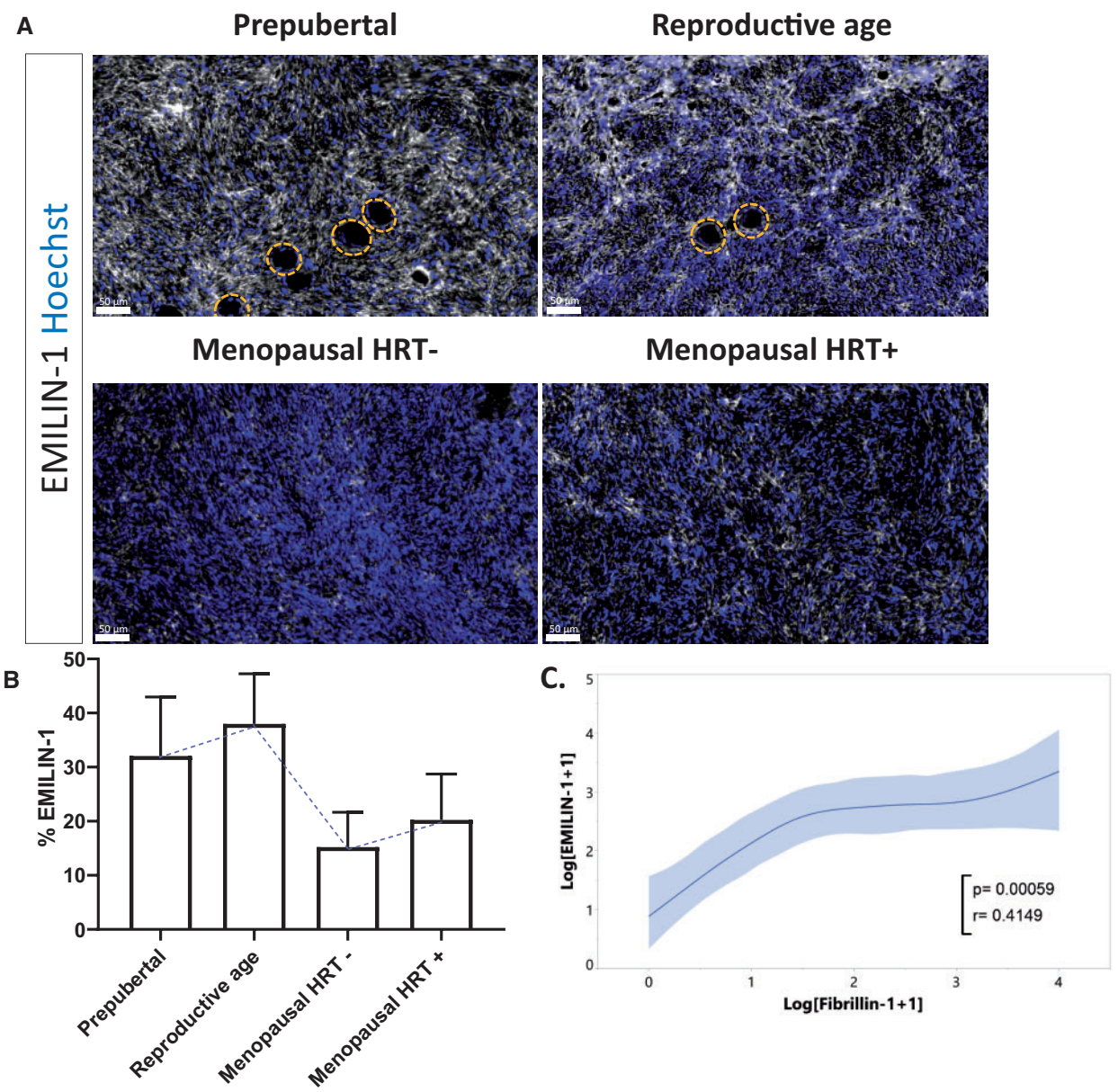


Figure 8 Spatiotemporal evolution of EMILIN-1 deposition in the ovarian interstitial ECM. (**A**) Immunofluorescent staining of tissue sections for EMILIN-1 (white) and counterstaining with Hoechst (blue) for nuclear observation. (**B**) At prepuberty, around 30% of the ovarian ECM surface area was found to be composed of EMILIN-1. This level increases slightly after puberty, only to decrease again at menopause. EMILIN-1 deposition is therefore not affected by HRT administration. (**C**) Positive correlation between EMILIN-1 and fibrillin-1. The represented data included analysis of ovarian tissue from 68 patients: prepubertal ($n = 16$); reproductive ($n = 21$); menopausal with estrogen-based HRT ($n = 7$); and menopausal without HRT ($n = 24$). The data plot fits a smoothing spline with a lambda value of 2.3. The curves also include the bootstrap confidence region for each fit generated by JMP® Pro 14.3.0. The Kruskal–Wallis (*post hoc*: Dunn) test was used to compare EMILIN-1 levels between age groups (*$P < 0.05$). Drawn circles highlight the presence of preantral follicles. Results are presented as mean ± SEM. Scale bars: 50 µm.

At the interface between elastin and fibrillin-1 (Colombatti *et al.*, 2000), EMILIN-1 plays a niche role in elastin fiber biogenesis by aiding with fusion of elastin fibers, making them more organized (Randell and Daneshtalab, 2017). EMILIN-1 was also detected in the human ovarian matrisome of adult patients by a proteomic approach (Ouni *et al.*, 2019), and recently in porcine ovarian tissue (Henning *et al.*, 2019). EMILIN-1 deposition is highly dependent on fibrillin-1 expression, as evidenced in fibrillin-1 knock-out mice, which were unable to synthesize EMILIN-1 (Schiavinato *et al.*, 2016). In view of these findings in mice and based on the weak but significant correlation established

Downloaded from https://academic.oup.com/humrep/article/35/6/1391/5857556 by UCLouvain-SCEB user on 13 June 2022

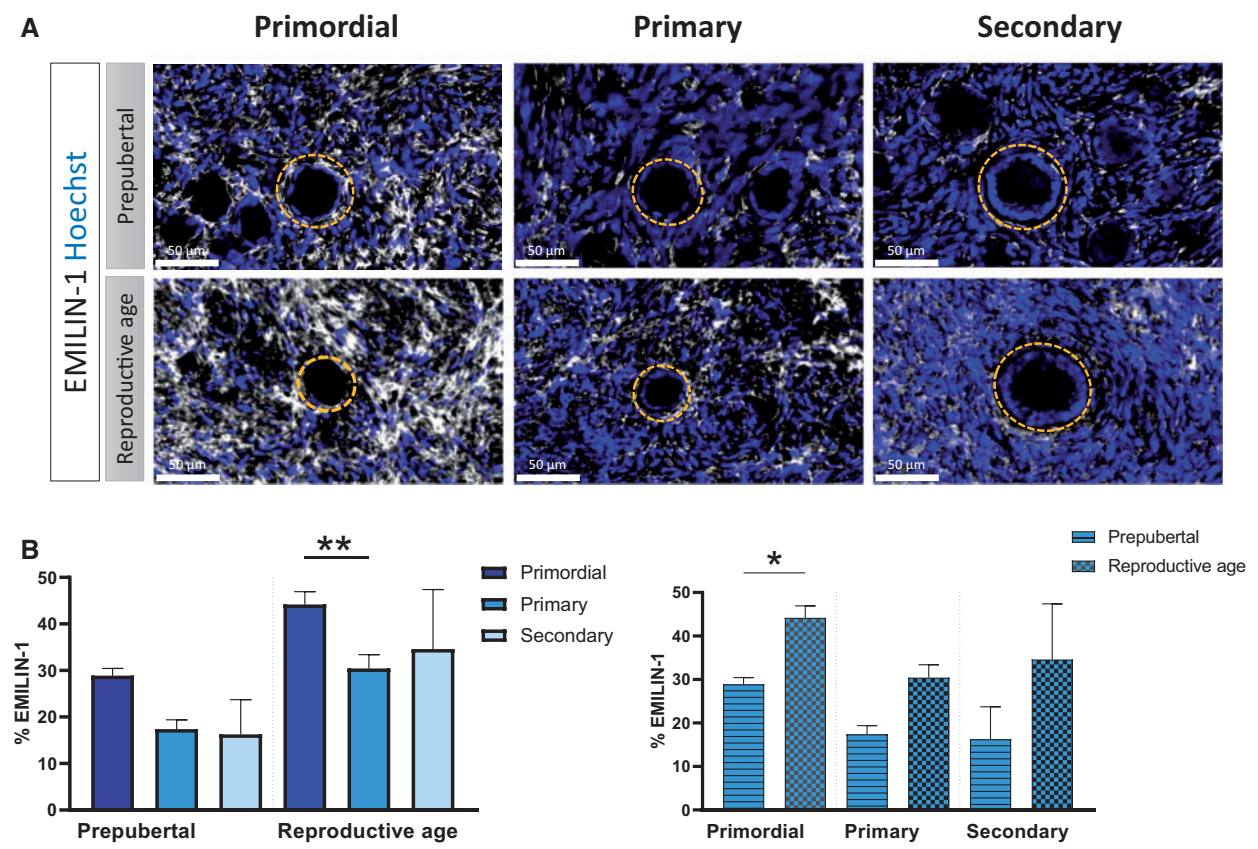


Figure 9 Comparison of EMILIN-1 distribution and deposition between prepubertal and reproductive-age perifollicular ECM during early folliculogenesis. (**A**) Immunofluorescent staining of tissue sections for fibrillin-1 (white) and counterstaining with Hoechst (blue) for nuclear observation. (**B**) In both prepubertal and reproductive-age patients, we observed a decrease in EMILIN-1 as folliculogenesis advanced. However, prepubertal perifollicular ECM showed the lowest EMILIN-1, especially at the primordial stage. The represented data included analysis of follicles from prepubertal ($n = 16$) and reproductive age tissues ($n = 21$). The comparison of perifollicular ECM at prepubertal versus reproductive age included primordial ($n = 826$ vs $n = 260$), primary ($n = 310$ vs $n = 198$) and secondary ($n = 25$ vs $n = 13$) follicles. The Kruskal–Wallis (*post hoc*: Dunn) test was used to compare EMILIN-1 levels between follicle stages in each group, and the Mann–Whitney test to compare prepubertal and reproductive-age follicles at the same developmental stage ($^*P < 0.05$, $^{**}P < 0.01$). Drawn circles highlight the presence of preantral follicles. Results are presented as mean ± SEM. Scale bars: 50 µm.

between EMILIN-1 and fibrillin-1, we can confirm the interdependence between EMILIN-1 and fibrillin-1 in the human ovary (Fig. 8C). Clearly, EMILIN-1 does not only depend on fibrillin-1 levels ($r = 0.4149$; $P = 0.00059$), but also other possible variables, such as age, menstrual phase and cellular signaling context (Kielty *et al.*, 2005; Wagenseil and Mecham, 2007; Colombatti *et al.*, 2011). Our results point to a lack of two fundamental elastogenesis-associated proteins (Shen *et al.*, 2016) at menopause, namely EMILIN-1 and fibrillin-1, which may produce elastic fiber abnormalities even after HRT, as explained by Zanetti *et al.* (2004).

Interestingly, both EMILIN-1 and fibrillin-1 serve as negative regulators of transforming growth factor beta (TGF-β) (Zacchigna *et al.*, 2006; Olivieri *et al.*, 2010). Consequently, and in line with the available literature, we can hypothesize that the growing lack of EMILIN-1 and fibrillin-1 in interstitial ovarian ECM with age may lead to an upturn in TGF-β (Isogai *et al.*, 2003; Neptune *et al.*, 2003; Zacchigna *et al.*, 2006), responsible for greater tissue rigidity and age-related fibrosis (Hayward and Brock, 1997; Briley *et al.*, 2016; McCloskey *et al.*, 2019).

All the elastic network components mentioned above are embedded in a hydrogel of GAG chain-containing proteoglycans (Frantz *et al.*, 2010). The innate polyanionic nature of GAGs is pivotal to maintaining water retention, hydrostatic pressure, nutrient transport, cell migration, cell differentiation, matrix structure and mechanical integrity (Kurylo *et al.*, 2016). From a mechanical point of view, GAGs enable healthy tissue to resist compressive stress thanks to their binding to fibrous ECM molecules (Scott, 2003). Thereby, GAGs act by inflating the collagen network and causing tensile stress that allows the ECM to resist shear deformation (Jin and Grodzinsky, 2001). Although a quantitative change in GAGs with age was expected, our data demonstrate maintenance of significantly higher GAG levels in adult ovaries than in prepubertal ones. In accordance with *in vitro* findings linking GAGs to disruption of fibrillin-1 aggregation (Kielty *et al.*, 1996; Tiedemann *et al.*, 2001), our *in vivo* study of GAG levels in human

Downloaded from https://academic.oup.com/humrep/article/35/6/1391/5857556 by UCLouvain-SCEB user on 13 June 2022

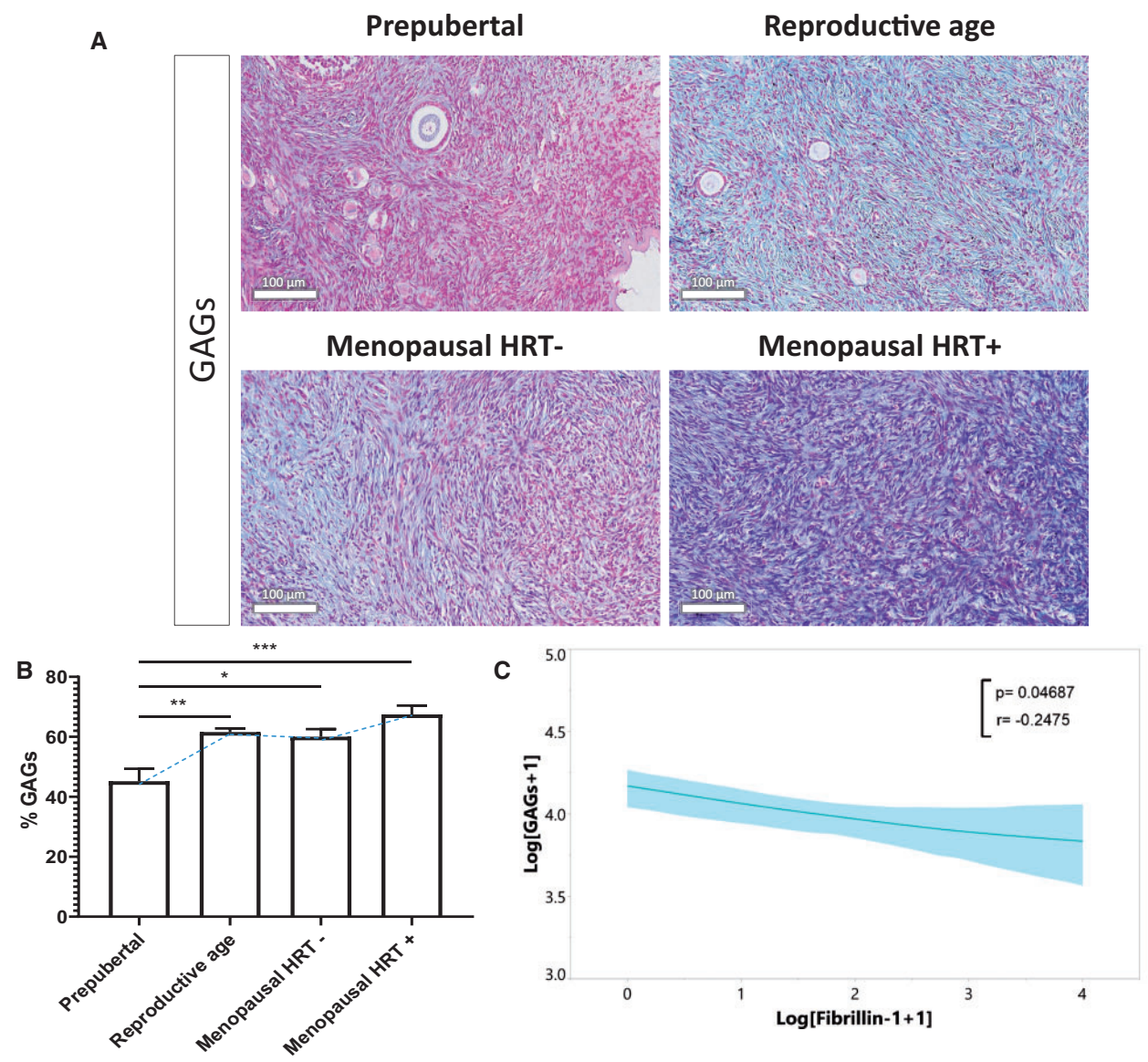


Figure 10 Age-dependent GAG accumulation in the ovarian interstitial ECM. (**A**) Alcian blue staining of sulfated and carboxylated GAGs (blue) in ovarian tissue, showing nuclear counterstaining with Mayer's carmalum (red). (**B**) Progressive accumulation of GAGs with age was observed within the interstitial ECM. (**C**) Negative correlation between GAGs and fibrillin-1. The data plot fits a smoothing spline with a lambda value of 2.3. The curves also include the bootstrap confidence region for each fit generated by JMP® Pro 14.3.0. The represented data included analysis of ovarian tissue from 68 patients: prepubertal ($n = 16$); reproductive ($n = 21$); menopausal with estrogen-based HRT ($n = 7$); and menopausal without HRT ($n = 24$). The Kruskal–Wallis (*post hoc*: Dunn) test was used to compare GAG levels between age groups (*$P < 0.05$, **$P < 0.01$ and ***$P < 0.001$). Results are presented as mean ± SEM. Scale bars: 100 µm.

ovaries revealed that the decrease in fibrillin-1 with age is weakly but significantly correlated to an increase in GAGs ($r = 0.2475$; $P = 0.04687$, Fig. 10C). This weak correlation indicates that fibrillin-1 and GAG deposition are dependent on other factors in the human ovary that require further investigation. More qualitative GAG studies are therefore needed to decipher the age-dependent effect on available GAG types in the ovary, which might further explain the GAG-fibrillin-1 interaction (Cain *et al.*, 2005).

Perifollicular ECM as a starting point for follicle development and biomechanical regulation

Our results showed perifollicular ECM changes with age to be very distinct from the rest of the interstitial ECM, which reinforces the dynamic reciprocity theory between ovarian follicles and their microenvironment (Woodruff and Shea, 2011; Thorne *et al.*, 2015).

Downloaded from https://academic.oup.com/humrep/article/35/6/1391/5857556 by UCLouvain-SCEB user on 13 June 2022

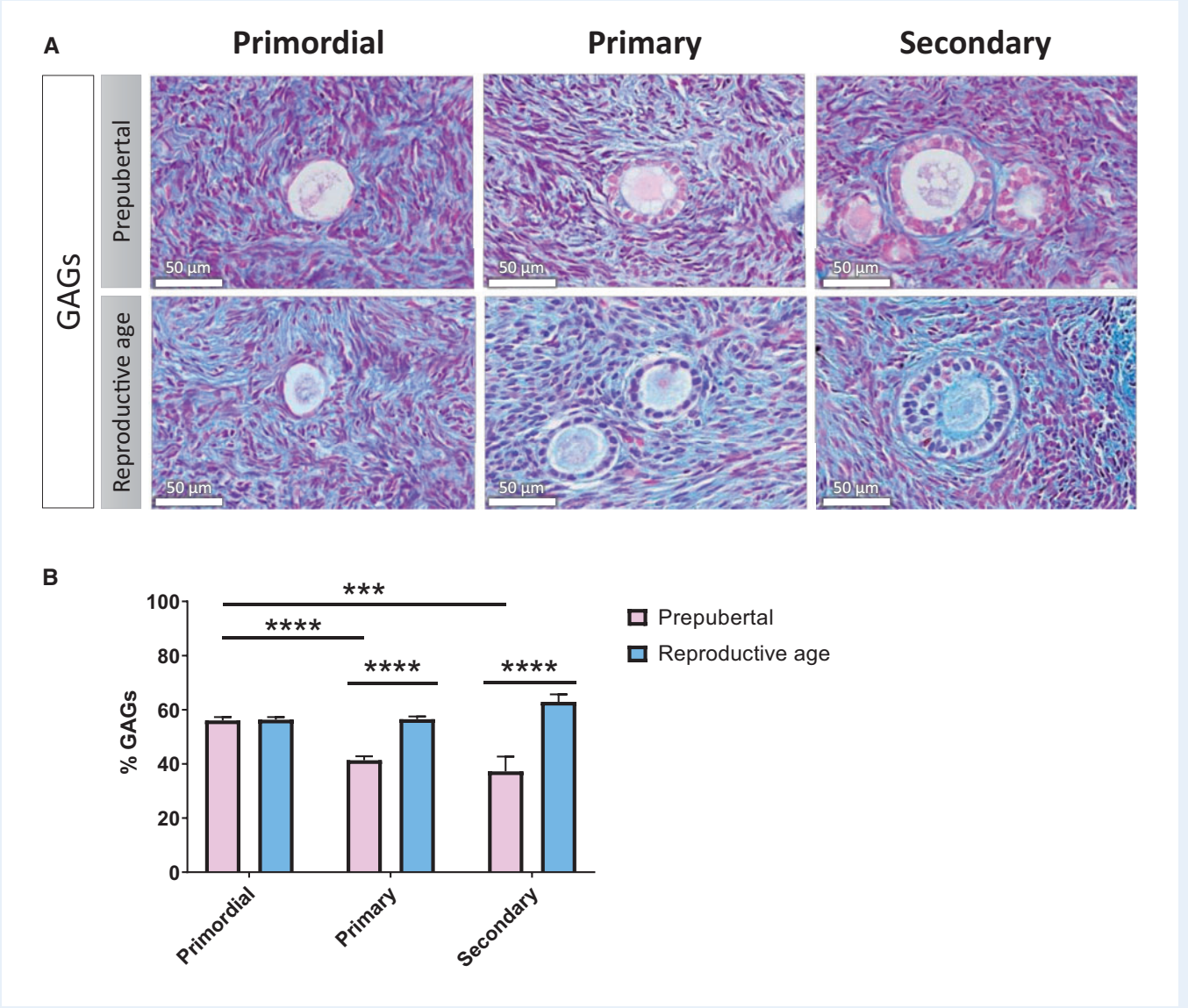


Figure 11 Comparison of GAG accumulation in the perifollicular ECM according to age and follicle stage. (**A**) Close-up of GAG content (blue) in the perifollicular ECM using Alcian blue staining. (**B**) While levels of GAGs fell significantly in the perifollicular microenvironment of prepubertal patients during early folliculogenesis, they remained stable at reproductive age from the primary to the secondary stage. Following follicle activation, the prepubertal perifollicular ECM was poorest in GAGs. (**C**) Negative correlation between GAGs and fibrillin-1 levels. The represented data included analysis of follicles from prepubertal ($n = 16$) and reproductive age tissues ($n = 21$). The comparison of perifollicular ECM at prepubertal versus reproductive age included primordial ($n = 217$ vs $n = 238$), primary ($n = 182$ vs $n = 160$) and secondary ($n = 18$ vs $n = 30$) follicles. Two-way ANOVA (*post hoc*: Tukey) was used to compare GAG content at all follicle stages in and between groups (***$P < 0.001$ and ****$P < 0.0001$). Results are presented as mean ± SEM. Scale bars: 50 µm.

Intriguingly, while higher collagen proportions were found in ovarian tissue from reproductive-age women than prepubertal girls, more collagen was actually accumulated in the ECM surrounding preantral follicles in the latter group. A closer look at fiber thickness by polarized light microscopy revealed that primordial follicles in prepubertal ovaries are surrounded by a higher proportion of thick collagen fibers. Thicker collagen fibers are less elastic and offer great resistance to tension forces, which could account for the preservation of primordial follicles in a resting state (Jorge *et al.*, 2014). After puberty, on the other hand, concomitant with the decrease in thicker fibers following follicle activation, there is a significant increase in thinner collagen fibers, probably due to enzymatic degradation. These findings highlight a profound difference in collagen deposition between young and adult perifollicular ECM, which is most pronounced in primordial follicles, and demonstrate that perifollicular ECM remodeling is vital for follicle growth (Hornick *et al.*, 2012). Elastin findings also support this theory, with perifollicular ECM showing less elastin deposition in prepubertal ovarian tissue at all follicle stages. Interestingly, in both groups, there is a

Downloaded from https://academic.oup.com/humrep/article/35/6/1391/5857556 by UCLouvain-SCEB user on 13 June 2022

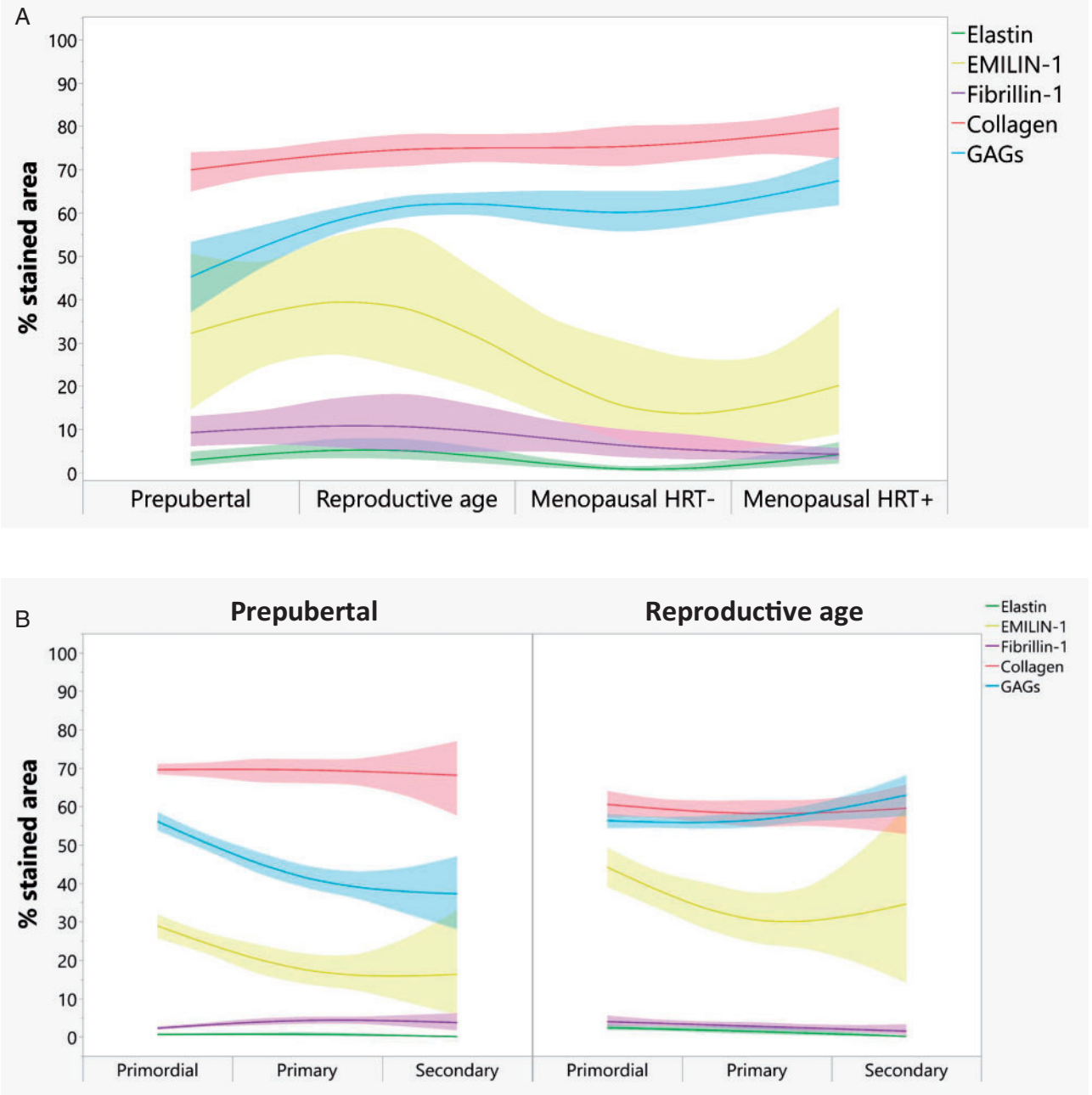


Figure 12 Summary of the spatiotemporal deposition of elastic matrisome components in the human ovary. (**A**) Summary of all studied elastic matrisome proteins in interstitial and (**B**) perifollicular ECM. The represented data included analysis of ovarian tissue from 68 patients: prepubertal ($n = 16$); reproductive ($n = 21$); menopausal with estrogen-based HRT ($n = 7$); and menopausal without HRT ($n = 24$). The curves represent average levels of the matrisome components in all groups and follicle stages at both prepuberty and reproductive age, fitting a smoothing spline with a lambda value of 0.05. The curves also include the bootstrap confidence region for each fit generated by JMP® Pro 14.3.0.

dramatic decline in this protein during follicle development from the primordial to the secondary stage, which is likely due to ECM digestion to support follicle growth. Whether based on collagen or elastin perifollicular ECM levels, our findings predict a stiffer microenvironment around prepubertal follicles, mainly at primordial and primary stages. These differences tend to diminish once follicles reach the secondary stage.

Besides their mechanical roles in ovarian tissue, fibrillin-1 and EMILIN-1 modulate important signaling pathways for ovarian homeostasis and follicle development (John *et al.*, 2008; Guo and Wang, 2009; Ernst *et al.*, 2017). EMILIN-1 is a negative regulator of cell proliferation (Colombatti *et al.*, 2011). Thus, the declining tendency of perifollicular EMILIN-1 levels with the progress of folliculogenesis in both prepubertal and reproductive age groups is consistent with granulosa

Downloaded from https://academic.oup.com/humrep/article/35/6/1391/5857556 by UCLouvain-SCEB user on 13 June 2022

cell proliferation in preantral follicles (Bax *et al.*, 2003; Conti and Chang, 2016). On the other hand, a lack of fibrillin-1 leads to tissue stiffening as a result of TGF-β signaling overactivation (MacFarlane *et al.*, 2017). Our findings and the available literature on folliculogenesis (McGee and Raj, 2015) suggest similar effects of fibrillin-1 in the ovary, pointing to a stiffer ECM around primordial follicles at prepuberty (Marque *et al.*, 2001; Alper, 2002; Kielty *et al.*, 2002; MacFarlane *et al.*, 2017; Abbas *et al.*, 2019). However, in prepubertal perifollicular ECM, there was a surge in fibrillin-1 after follicle activation, which was not observed in adult tissue. This might suggest ECM remodeling by way of increasing its elasticity and releasing growing follicles from their mechanical retention (Woodruff and Shea, 2011; Nagamatsu *et al.*, 2019). Knowing that GAGs also contribute to tissue elasticity, comparison of GAGs in perifollicular ECM revealed lower levels of GAGs surrounding prepubertal follicles, which complements our theory of greater mechanical retention of prepubertal follicles. Although we did not observe significant changes in GAG levels in reproductive-age tissue during the same period, we cannot exclude the possibility of qualitative GAG differences (Hatzirodos *et al.*, 2012; Takahashi *et al.*, 2014) between ages and follicular stages, calling for further GAGOme studies (Chen *et al.*, 2018).

Taken together, these results clearly illustrate ECM deposition and remodeling in an age- and follicle stage-related manner (Fig. 12, Supplementary Video and Fig. S5). More precisely, our findings point to a more elastic ECM surrounding reproductive-age follicles compared to the less compliant perifollicular ECM of prepubertal tissue. However, menstrual cycle phase and age-related changes to the stroma, follicle density and vascularization can also impact ECM composition. Advanced combinational analysis will therefore be needed in the future to calculate the contribution of each matrisome component to ovarian plasticity.

In conclusion, from a biochemical perspective, our study revealed interesting changes to ECM composition, dictating the elastic features of ovarian tissue, in line with the existing literature. Our findings pave the way for possible therapeutic targets at the ECM level in the context of female fertility and ovarian rejuvenation. Our data will prove very useful in designing biomimetic scaffolds and tissue-engineered models, such as the artificial ovary (Amorim and Shikanov, 2016; Dolmans and Amorim, 2019). Indeed, they emphasize the importance of encapsulating each type of isolated follicle in an appropriate biomaterial that must replicate the corresponding functional perifollicular ECM and respect ovarian tissue heterogeneity (Choi *et al.*, 2014) to guarantee its biomimicry. Although our data disclose the complexity of this task, they also offer new opportunities to explore ovarian ECM synthesis *de novo*, which may reverse ovarian aging, and help us to develop reliable *in vitro* models to complement our knowledge of human ovary regulation.

Supplementary data

Supplementary data are available at *Human Reproduction* online.

Acknowledgments

We thank Olivier Van Kerk and Sarah Storder for their technical assistance, as well as Thuy Tran and Soulaima Cherkaoui for their contribution to experimental procedures. We also thank Lieven Desmet (Louvain Institute of Data Analysis and Modeling in Economics and Statistics, Université Catholique de Louvain) for his advice on biostatistical evaluation, and Mira Hryniuk, BA, for reviewing the English language of the manuscript. Holotomography acquisitions were achieved thanks to the invaluable contribution of Sanela Vellino and Thibault Courthéoux from Nanolive. Finally, we are very grateful to Omar Rhouma for graphic illustration.

Authors' roles

E.O.: conception and design, experimental procedures, analysis of results and article preparation; C.B.: design of digital image analysis; M.M.D.: clinical inspection of patient records and critical manuscript revision; E.M.: inspection of histological descriptions and classifications; S.P.D.R.: text-mining; D.V.: critical manuscript revision from a proteomic point of view; and C.A.A.: conception and design, discussion contribution and critical manuscript revision.

Funding

This study was supported by grants from the Fonds National de la Recherche Scientifique de Belgique (FNRS) (C.A.A. is an FRS-FNRS research associate; grant 5/4/150/5 awarded to M.M.D.) and the Université Catholique de Louvain (PhD grant 'Coopération au développement' awarded to E.O.).

Conflict of interest

The authors report no conflict of interest and have nothing to disclose.

References

Abbas Y, Carnicer-Lombarte A, Gardner L, Thomas J, Brosens JJ, Moffett A, Sharkey AM, Franze K, Burton GJ, Oyen ML. Tissue stiffness at the human maternal-fetal interface. *Hum Reprod* 2019; **34**:1999–2008.

Aboubakar Nana F, Hoton D, Ambroise J, Lecocq M, Vanderputten M, Sibille Y, Vanaudenaerde B, Pilette C, Bouzin C, Ocak S. Increased expression and activation of FAK in small-cell lung cancer compared to non-small-cell lung cancer. *Cancers* 2019;**11**: 1526.

Adhikari D, Liu K. Molecular mechanisms underlying the activation of mammalian primordial follicles. *Endocr Rev* 2009;**30**:438–464.

Afratis N, Gialeli C, Nikitovic D, Tsegenidis T, Karousou E, Theocharis AD, Pavao MS, Tzanakakis GN, Karamanos NK. Glycosaminoglycans: key players in cancer cell biology and treatment. *FEBS J* 2012;**279**:1177–1197.

Alper J. Protein structure. Stretching the limits. *Science* 2002;**297**: 329–331.

Amorim CA, Shikanov A. The artificial ovary: current status and future perspectives. *Future Oncol* 2016;**12**:2323–2332.

Bastian NA, Bayne RA, Hummitzsch K, Hatzirodos N, Bonner WM, Hartanti MD, Irving-Rodgers HF, Anderson RA, Rodgers RJ. Regulation of fibrillins and modulators of TGFbeta in fetal bovine and human ovaries. *Reproduction* 2016;**152**:127–137.

Downloaded from https://academic.oup.com/humrep/article/35/6/1391/5857556 by UCLouvain-SCEB user on 13 June 2022

Bax DV, Bernard SE, Lomas A, Morgan A, Humphries J, Shuttleworth CA, Humphries MJ, Kielty CM. Cell adhesion to fibrillin-1 molecules and microfibrils is mediated by alpha 5 beta 1 and alpha v beta 3 integrins. *J Biol Chem* 2003;**278**:34605–34616.

Briley SM, Jasti S, McCracken JM, Hornick JE, Fegley B, Pritchard MT, Duncan FE. Reproductive age-associated fibrosis in the stroma of the mammalian ovary. *Reproduction* 2016;**152**:245–260.

Cain SA, Baldock C, Gallagher J, Morgan A, Bax DV, Weiss AS, Shuttleworth CA, Kielty CM. Fibrillin-1 interactions with heparin. Implications for microfibril and elastic fiber assembly. *J Biol Chem* 2005;**280**:30526–30537.

Chen YH, Narimatsu Y, Clausen TM, Gomes C, Karlsson R, Steentoft C, Spliid CB, Gustavsson T, Salanti A, Persson A *et al*. The GAGOme: a cell-based library of displayed glycosaminoglycans. *Nat Methods* 2018;**15**:881–888.

Choi JK, Agarwal P, Huang H, Zhao S, He X. The crucial role of mechanical heterogeneity in regulating follicle development and ovulation with engineered ovarian microtissue. *Biomaterials* 2014;**35**:5122–5128.

Colombatti A, Doliana R, Bot S, Canton A, Mongiat M, Mungiguerra G, Paron-Cilli S, Spessotto P. The EMILIN protein family. *Matrix Biol* 2000;**19**:289–301.

Colombatti A, Spessotto P, Doliana R, Mongiat M, Bressan GM, Esposito G. The EMILIN/multimerin family. *Front Immunol* 2011;**2**:93.

Conti M, Chang RJ. Folliculogenesis, ovulation, and luteogenesis. In J Larry Jameson, DM de Kretser, LC Giudice, AB Grossman, S Melmed, JT Potts, GC Weir (ed). *Endocrinology: Adult and Pediatric*. 7th edn. Philadelphia, USA: Elsevier, 2016, 2179–2191.e2173.

Dayan D, Hiss Y, Hirshberg A, Bubis JJ, Wolman M. Are the polarization colors of picrosirius red-stained collagen determined only by the diameter of the fibers? *Histochemistry* 1989;**93**:27–29.

Dolmans MM, Amorim CA. Construction and use of artificial ovaries. *Reproduction* 2019;**158**:F15-F25.

Ernst EH, Grondahl ML, Grund S, Hardy K, Heuck A, Sunde L, Franks S, Andersen CY, Villesen P, Lykke-Hartmann K. Dormancy and activation of human oocytes from primordial and primary follicles: molecular clues to oocyte regulation. *Hum Reprod* 2017;**32**:1684–1700.

Filatov M, Khramova Y, Parshina E, Bagaeva T, Semenova M. Influence of gonadotropins on ovarian follicle growth and development in vivo and in vitro. *Zygote* 2017;**25**:235–243.

Ford E, Beckett EL, Roman S, McLaughlin EA, Sutherland J. Advances in human primordial follicle activation and premature ovarian insufficiency. *Reproduction* 2020;**159**:R15-R29.

Frantz C, Stewart KM, Weaver VM. The extracellular matrix at a glance. *J Cell Sci* 2010;**123**:4195–4200.

Grive KJ, Freiman RN. The developmental origins of the mammalian ovarian reserve. *Development* 2015;**142**:2554–2563.

Guo X, Wang XF. Signaling cross-talk between TGF-beta/BMP and other pathways. *Cell Res* 2009;**19**:71–88.

Hatzirodos N, Nigro J, Irving-Rodgers HF, Vashi AV, Hummitzsch K, Caterson B, Sullivan TR, Rodgers RJ. Glycomic analyses of ovarian follicles during development and atresia. *Matrix Biol* 2012;**31**:45–56.

Hayat MA. *Stains and Cytochemical Methods*. 1st edn. New York, USA: Plenum Press, 1993.

Hayward C, Brock DJ. Fibrillin-1 mutations in Marfan syndrome and other type-1 fibrillinopathies. *Hum Mutat* 1997;**10**:415–423.

Henning NF, LeDuc RD, Even KA, Laronda MM. Proteomic analyses of decellularized porcine ovaries identified new matrisome proteins and spatial differences across and within ovarian compartments. *Sci Rep* 2019;**9**:20001.

Hornick JE, Duncan FE, Shea LD, Woodruff TK. Isolated primate primordial follicles require a rigid physical environment to survive and grow in vitro. *Hum Reprod* 2012;**27**:1801–1810.

Hsueh AJ, Kawamura K, Cheng Y, Fauser BC. Intraovarian control of early folliculogenesis. *Endocr Rev* 2015;**36**:1–24.

Isogai Z, Ono RN, Ushiro S, Keene DR, Chen Y, Mazzieri R, Charbonneau NL, Reinhardt DP, Rifkin DB, Sakai LY. Latent transforming growth factor beta-binding protein 1 interacts with fibrillin and is a microfibril-associated protein. *J Biol Chem* 2003;**278**:2750–2757.

Jin M, Grodzinsky AJ. Effect of electrostatic interactions between glycosaminoglycans on the shear stiffness of cartilage: a molecular model and experiments. *Macromolecules* 2001;**34**:8330–8339.

John GB, Gallardo TD, Shirley LJ, Castrillon DH. Foxo3 is a PI3K-dependent molecular switch controlling the initiation of oocyte growth. *Dev Biol* 2008;**321**:197–204.

Jorge S, Chang S, Barzilai JJ, Leppert P, Segars JH. Mechanical signaling in reproductive tissues: mechanisms and importance. *Reprod Sci* 2014;**21**:1093–1107.

Kawamura K, Cheng Y, Suzuki N, Deguchi M, Sato Y, Takae S, Ho CH, Kawamura N, Tamura M, Hashimoto S *et al*. Hippo signaling disruption and Akt stimulation of ovarian follicles for infertility treatment. *Proc Natl Acad Sci USA* 2013;**110**:17474–17479.

Kawamura K, Kawamura N, Hsueh AJ. Activation of dormant follicles: a new treatment for premature ovarian failure? *Curr Opin Obstet Gynecol* 2016;**28**:217–222.

Kawashima I, Kawamura K. Regulation of follicle growth through hormonal factors and mechanical cues mediated by Hippo signaling pathway. *Syst Biol Reprod Med* 2018;**64**:3–11.

Kielty CM, Sherratt MJ, Marson A, Baldock C. Fibrillin microfibrils. *Adv Protein Chem* 2005;**70**:405–436.

Kielty CM, Sherratt MJ, Shuttleworth CA. Elastic fibres. *J Cell Sci* 2002;**115**:2817–2828.

Kielty CM, Whittaker SP, Shuttleworth CA. Fibrillin: evidence that chondroitin sulphate proteoglycans are components of microfibrils and associate with newly synthesised monomers. *FEBS Lett* 1996;**386**:169–173.

Kiernan JA. Dyes and other colorants in microtechnique and biomedical research. *Color Technol* 2006;**122**:1–21.

Kurylo MP, Grandfield K, Marshall GW, Altoe V, Aloni S, Ho SP. Effect of proteoglycans at interfaces as related to location, architecture, and mechanical cues. *Arch Oral Biol* 2016;**63**:82–92.

Lescan M, Perl RM, Golombek S, Pilz M, Hann L, Yasmin M, Behring A, Keller T, Nolte A, Gruhn F *et al*. De novo synthesis of elastin by exogenous delivery of synthetic modified mRNA into skin and elastin-deficient cells. *Mol Ther Nucleic Acids* 2018;**11**:475–484.

Levillain A, Orhant M, Turquier F, Hoc T. Contribution of collagen and elastin fibers to the mechanical behavior of an abdominal connective tissue. *J Mech Behav Biomed Mater* 2016;**61**:308–317.

Lunde O, Djoseland O, Grottum P. Polycystic ovarian syndrome: a follow-up study on fertility and menstrual pattern in 149 patients

Downloaded from https://academic.oup.com/humrep/article/35/6/1391/5857556 by UCLouvain-SCEB user on 13 June 2022

15-25 years after ovarian wedge resection. *Hum Reprod* 2001;**16**: 1479–1485.

MacFarlane EG, Haupt J, Dietz HC, Shore EM. TGF-beta family signaling in connective tissue and skeletal diseases. *Cold Spring Harb Perspect Biol* 2017;**9**:a022269.

MacKenna DA, Omens JH, McCulloch AD, Covell JW. Contribution of collagen matrix to passive left ventricular mechanics in isolated rat hearts. *Am J Physiol* 1994;**266**:H1007–H1018.

Malandrino A, Mak M, Kamm RD, Moeendarbary E. Complex mechanics of the heterogeneous extracellular matrix in cancer. *Extreme Mech Lett* 2018;**21**:25–34.

Mammoto T, Mammoto A, Ingber DE. Mechanobiology and developmental control. *Annu Rev Cell Dev Biol* 2013;**29**:27–61.

Marque V, Kieffer P, Gayraud B, Lartaud-Idjouadiene I, Ramirez F, Atkinson J. Aortic wall mechanics and composition in a transgenic mouse model of Marfan syndrome. *Arterioscler Thromb Vasc Biol* 2001;**21**:1184–1189.

McCloskey CW, Cook DP, Kelly BS, Azzi F, Allen CH, Forsyth A, Upham J, Rayner KJ, Gray DA, Boyd RW *et al*. Metformin abrogates age-associated ovarian fibrosis. *Clin Cancer Res* 2020;**26**: 632–642.

McGee EA, Raj RS. Regulators of ovarian preantral follicle development. *Semin Reprod Med* 2015;**33**:179–184.

Nagamatsu G, Shimamoto S, Hamazaki N, Nishimura Y, Hayashi K. Mechanical stress accompanied with nuclear rotation is involved in the dormant state of mouse oocytes. *Sci Adv* 2019;**5**:eaav9960.

Neptune ER, Frischmeyer PA, Arking DE, Myers L, Bunton TE, Gayraud B, Ramirez F, Sakai LY, Dietz HC. Dysregulation of TGF-beta activation contributes to pathogenesis in Marfan syndrome. *Nat Genet* 2003;**33**:407–411.

Olivieri J, Smaldone S, Ramirez F. Fibrillin assemblies: extracellular determinants of tissue formation and fibrosis. *Fibrogenesis Tissue Repair* 2010;**3**:24.

Oomen PJA, Holland MA, Bouten CVC, Kuhl E, Loerakker S. Growth and remodeling play opposing roles during postnatal human heart valve development. *Sci Rep* 2018;**8**:1235.

Ouni E, Vertommen D, Chiti MC, Dolmans MM, Amorim CA. A draft map of the human ovarian proteome for tissue engineering and clinical applications. *Mol Cell Proteomics* 2019;**18**:S159–S173.

Randell A, Daneshtalab N. Elastin microfibril interface-located protein 1, transforming growth factor beta, and implications on cardiovascular complications. *J Am Soc Hypertens* 2017;**11**:437–448.

Rich L, Whittaker P. Collagen and picrosirius red staining: a polarized light assessment of fibrillar hue and spatial distribution. *Braz J morphol Sci* 2005;**2**:97–104.

Sanada H, Shikata J, Hamamoto H, Ueba Y, Yamamuro T, Takeda T. Changes in collagen cross-linking and lysyl oxidase by estrogen. *Biochim Biophys Acta* 1978;**541**:408–413.

Schiavinato A, Keene DR, Wohl AP, Corallo D, Colombatti A, Wagener R, Paulsson M, Bonaldo P, Sengle G. Targeting of EMILIN-1 and EMILIN-2 to fibrillin microfibrils facilitates their incorporation into the extracellular matrix. *J Invest Dermatol* 2016; **136**:1150–1160.

Schindelin J, Arganda-Carreras I, Frise E, Kaynig V, Longair M, Pietzsch T, Preibisch S, Rueden C, Saalfeld S, Schmid B *et al*. Fiji: an open-source platform for biological-image analysis. *Nat Methods* 2012;**9**:676–682.

Scott JE. Elasticity in extracellular matrix 'shape modules' of tendon, cartilage, etc. A sliding proteoglycan-filament model. *J Physiol* 2003; **553**:335–343.

Shah JS, Sabouni R, Cayton Vaught KC, Owen CM, Albertini DF, Segars JH. Biomechanics and mechanical signaling in the ovary: a systematic review. *J Assist Reprod Genet* 2018;**35**:1135–1148.

Shen S, Hinderer S, Schenke-Layland K. Scaffold and biomechanical transductive approaches to elastic tissue engineering. In CK Anand Ramamurthi (ed). *Elastic Fiber Matrices*. Boca Raton, USA: CRC Press, 2016, 24.

Swee MH, Parks WC, Pierce RA. Developmental regulation of elastin production. Expression of tropoelastin pre-mRNA persists after down-regulation of steady-state mRNA levels. *J Biol Chem* 1995; **270**:14899–14906.

Takahashi N, Tarumi W, Ishizuka B. Involvement of hyaluronan synthesis in ovarian follicle growth in rats. *Reproduction* 2014;**147**: 189–197.

Thorne JT, Segal TR, Chang S, Jorge S, Segars JH, Leppert PC. Dynamic reciprocity between cells and their microenvironment in reproduction. *Biol Reprod* 2015;**92**:25.

Tiedemann K, Batge B, Muller PK, Reinhardt DP. Interactions of fibrillin-1 with heparin/heparan sulfate, implications for microfibrillar assembly. *J Biol Chem* 2001;**276**:36035–36042.

Wagenseil JE, Mecham RP. New insights into elastic fiber assembly. *Birth Defects Res C Embryo Today* 2007;**81**:229–240.

Wood CD, Vijayvergia M, Miller FH, Carroll T, Fasanati C, Shea LD, Brinson LC, Woodruff TK. Multi-modal magnetic resonance elastography for noninvasive assessment of ovarian tissue rigidity in vivo. *Acta Biomater* 2015;**13**:295–300.

Woodruff TK, Shea LD. A new hypothesis regarding ovarian follicle development: ovarian rigidity as a regulator of selection and health. *J Assist Reprod Genet* 2011;**28**:3–6.

Xu M, West E, Shea LD, Woodruff TK. Identification of a stage-specific permissive in vitro culture environment for follicle growth and oocyte development. *Biol Reprod* 2006;**75**:916–923.

Zacchigna L, Vecchione C, Notte A, Cordenonsi M, Dupont S, Maretto S, Cifelli G, Ferrari A, Maffei A, Fabbro C *et al*. Emilin1 links TGF-beta maturation to blood pressure homeostasis. *Cell* 2006;**124**:929–942.

Zanetti M, Braghetta P, Sabatelli P, Mura I, Doliana R, Colombatti A, Volpin D, Bonaldo P, Bressan GM. EMILIN-1 deficiency induces elastogenesis and vascular cell defects. *Mol Cell Biol* 2004;**24**: 638–650.

Downloaded from https://academic.oup.com/humrep/article/35/6/1391/5857556 by UCLouvain-SCEB user on 13 June 2022